U.S. DEPARTMENT OF THE INTERIOR
U.S. GEOLOGICAL SURVEY

TO ACCOMPANY MAP CP-44

EXPLANATORY NOTES FOR THE MINERAL-RESOURCES MAP OF THE CIRCUM-PACIFIC REGION SOUTHEAST QUADRANT

1:10,000,000

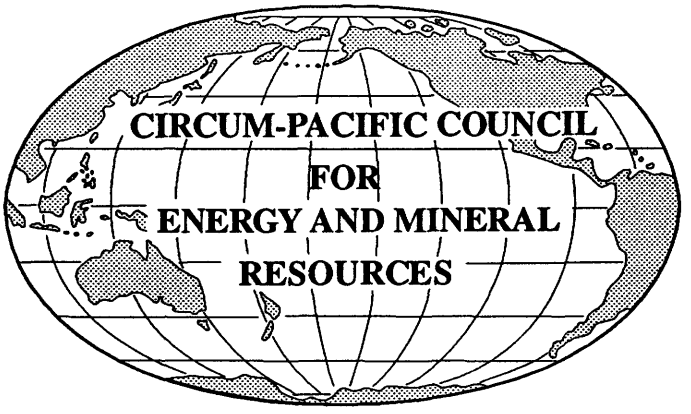

1996

CIRCUM-PACIFIC COUNCIL FOR ENERGY AND MINERAL RESOURCES
Michel T. Halbouty, Chair

CIRCUM-PACIFIC MAP PROJECT
John A. Reinemund, Director
George Gryc, General Chair
Philip W. Guild, Advisor
Mineral-Resources Map Series

EXPLANATORY NOTES FOR THE MINERAL-RESOURCES MAP OF THE CIRCUM-PACIFIC REGION SOUTHEAST QUADRANT

1:10,000,000

By

José Corvalán D., Servicio Nacional de Geología y Minería, Santiago, Chile

Alirio Bellizzia and **Nelly Pimentel**, Dirección General de Geología, Ministerio de Energía y Minas, Caracas, Venezuela

Joaquín Buenaventura, Instituto Nacional de Investigaciones Geológico-Mineras, Bogota, Colombia

David Z. Piper, Theresa R. Swint-Iki, Gretchen Luepke, and **George Gryc,** U.S. Geological Survey, Menlo Park, California 94025, U.S.A.

Floyd W. McCoy, University of Hawaii, Kaneohe, Hawaii 96744, U.S.A.

Frank T. Manheim and **Candice M. Lane-Bostwick,** U.S. Geological Survey, Woods Hole, Massachusetts 02543, U.S.A.

1996

Explanatory Notes to Supplement the

MINERAL-RESOURCES MAP OF THE CIRCUM-PACIFIC REGION SOUTHEAST QUADRANT

José Corvalán D., Chair
Southeast Quadrant Panel

LAND RESOURCES

José Corvalán D., Servicio Nacional de Geología y Minería, Santiago, Chile

Philip W. Guild, U.S. Geological Survey, Reston, Virginia 22092, U.S.A.

SEAFLOOR RESOURCES

David Z. Piper, Theresa R. Swint-Iki, and **Gretchen Luepke,** U.S. Geological Survey, Menlo Park, California 94025, U.S.A.

Floyd W. McCoy, University of Hawaii, Kaneohe, Hawaii 96744, U.S.A.

Lawrence G. Sullivan, Lamont-Doherty Earth Observatory, Palisades, New York 10964, U.S.A.

Frank T. Manheim and **Candice M. Lane-Bostwick,** U.S. Geological Survey, Woods Hole, Massachusetts 02543, U.S.A.

Map compilation coordinated by
George Gryc
U.S. Geological Survey
Menlo Park, California 94025, U.S.A.

CONTENTS

INTRODUCTION

By
George Gryc

CIRCUM-PACIFIC MAP PROJECT

The Circum-Pacific Map Project is a cooperative international effort designed to show the relations of known energy and mineral resources to the major geologic features of the Pacific Basin and surrounding continental areas. Available geologic, mineral-resource, and energy-resource data are being integrated with new project-developed data sets such as magnetic lineations, seafloor mineral deposits, and seafloor sediment. Earth scientists representing some 180 organizations from more than 40 Pacific-region countries are involved in this work.

Six overlapping equal-area regional maps at a scale of 1:10,000,000 form the cartographic base for the project: the four Circum-Pacific Quadrants (Northwest, Southwest, Southeast, and Northeast), and the Antarctic and Arctic Sheets. There is also a Pacific Basin Sheet at a scale of 1:17,000,000. Published map series include the Base (published from 1977 to 1989), the Geographic (published from 1977 to 1990), the Geodynamic (published from 1984 to 1990), and the Plate-Tectonic (published from 1981 to 1992); all of them include seven map sheets. Thematic map series in the process of completing publication include Geologic (publication initiated in 1983), Tectonic (publication initiated in 1991), Energy-Resources (publication initiated in 1986), and Mineral-Resources (publication initiated in 1984). Altogether, 57 map sheets are planned. The maps are prepared cooperatively by the Circum-Pacific Council for Energy and Mineral Resources and the U.S. Geological Survey. Maps published prior to mid-1990 are distributed by the American Association of Petroleum Geologists (AAPG) Bookstore, P.O. Box 979, Tulsa, Oklahoma 74101, U.S.A.; maps published from mid-1990 onward are available from the Branch of Distribution, U.S. Geological Survey, Box 25286, Federal Center, Denver, Colorado 80225, U.S.A.

The Circum-Pacific Map Project is organized under six panels of geoscientists representing national earth-science organizations, universities, and natural-resource companies. The regional panels correspond to the basic map areas. Current panel chairs are Tomoyuki Moritani (Northwest Quadrant), R.W. Johnson (Southwest Quadrant), Ian W.D. Dalziel (Antarctic Region), José Corvalán D. (Southeast Quadrant), Kenneth J. Drummond (Northeast Quadrant), and George W. Moore (Arctic Region).

Project coordination and final cartography are being carried out through the cooperation of the Office of International Geology of the U.S. Geological Survey under the direction of Map Project General Chair George Gryc of Menlo Park, California, with the assistance of Warren O. Addicott, consultant. Project headquarters are located at 345 Middlefield Road, MS 952, Menlo Park, California 94025, U.S.A. The project has been overseen from its inception by John A. Reinemund, Director of the Map Project since 1982.

The framework for the Circum-Pacific Map Project was developed in 1973 by a specially convened group of 12 North American geoscientists meeting in California. The project was officially launched at the First Circum-Pacific Conference on Energy and Mineral Resources, held in Honolulu, Hawaii, in August 1974. Sponsors of the conference were the American Association of Petroleum Geologists (AAPG), Pacific Science Association (PSA), and the Committee for Coordination of Joint Prospecting for Mineral Resources in East Asian Offshore Areas (CCOP). The Circum-Pacific Map Project operates as an activity of the Circum-Pacific Council for Energy and Mineral Resources, a nonprofit organization that promotes cooperation among Circum-Pacific countries in the study of energy and mineral resources of the Pacific Basin. Founded by Michel T. Halbouty in 1972, the Council also sponsors quadrennial conferences, topical symposia, scientific training seminars, and the Earth Science Series of publications.

Published thematic maps of the Southeast Quadrant include the Plate-Tectonic Map (Corvalán, 1982), the Geodynamic Map (Corvalán, 1985a), the Geologic Map (Corvalán, 1985b), and the Energy-Resources Map (Yrigoyen and others, 1991). The Tectonic Map is now in cartographic preparation at Circum-Pacific Map Project headquarters in Menlo Park, California.

MINERAL-RESOURCES MAP SERIES

The Mineral-Resources Map Series is designed to be as factual as possible, with a minimum of interpretation. The small scale, 100 km/cm or 10,000 km^2/cm^2 (about 160 miles per inch or 25,000 square miles per square inch), requires an enormous simplification of both the background information and the mineral-deposit data; hence, the maps can give only a general impression of the distribution, character, and geologic environment of these resources. Nevertheless, this map series provides a unified overview of the mineral resources of a region encompassing more than half the globe. It identifies favorable areas for the occurrence of specific minerals and thus assists both in resource assessment and, with additional data from more detailed sources, in exploration planning. The maps also serve to show the relation of deposits to major earth features, such as divergent and convergent plate margins, hotspots, and accreted terranes, and thus should stimulate analysis of the role of geologic processes in the genesis of ores.

The maps show both land and seafloor deposits of most metallic and nonmetallic minerals, except for construction materials. Uranium and thorium are included, although their principal use is for energy production. Deposits on land are shown regardless of

their status of exploitation, and some deposits may have been totally exhausted. The maps do not, therefore, necessarily represent the present resource picture. In general, only deposits of economic size and grade are shown, but some small or low-grade occurrences have been included, where space permits, in order to indicate a resource potential. Deposits on land are shown by colored symbols outlined in black that are explained in detail on the map.

Because most seafloor deposits have not been evaluated for their economic potential, the criterion for their inclusion on the map sheets is simply knowledge of their existence. Reported occurrences of nearshore heavy minerals (placer deposits) are indicated by chemical symbols (letters) in blue.

Offshore mineral resources depicted are (1) manganese-iron oxide nodules that contain varying amounts of nickel, copper, and cobalt, and trace amounts of other metals; (2) sulfide deposits; and (3) phosphatic deposits. No attempt has been made to show the distribution of metalliferous sediment, which is known to be widespread but generally is so low in grade that it is not considered to be resources at the present time (Field and others, 1981).

Mineral-resource information for the land and near-shore (placer) areas is assembled by members of the individual quadrant panels; compilers, contributors, and data sources are cited on the maps themselves. Information on the offshore resources has been assembled for the entire ocean area of the project, principally by geologists of the U.S. Geological Survey.

The geologic features on the Mineral-Resources Maps are taken from the corresponding geologic maps, but are in general simplified and in part modified to emphasize features that may be significant in explaining the distribution of the mineral deposits. Although the project aims at a uniform presentation throughout the Circum-Pacific region, differences among the compilers in interpretation of its geologic evolution may result in some variation in the representation of the background information of land areas from map to map. Similarly, the method of representing land-based mineral deposits varies somewhat to reflect the views of the compilers.

The only exception is Antarctica, where no economically minable deposits are known; the criteria for inclusion on that map have been relaxed to show mineral occurrences without regard to their grade or their size (shown on the map as small).

Bathymetry and the nature of surficial sediment constitute the background for the oceanic areas. The 4 types of surficial sediment shown are simpified from 13 categories shown in the Geologic Map Series (McCoy, 1985). Active plate boundaries are taken from the Plate-Tectonic Map Series (Moore, 1982), but spreading axes are depicted as lines of uniform width rather than of varying widths reflecting spreading rates.

MINERAL-RESOURCES MAP OF THE SOUTHEAST QUADRANT

The Mineral-Resources Map of the Southeast Quadrant of the Circum-Pacific Region is the third published in a series of six overlapping 1:10,000,000-scale Mineral-Resources Maps. The Northeast Quadrant Mineral-Resources Map (Drummond) was published in 1985, and the Southwest Quadrant Mineral-Resources Map (Palfreyman) in 1995.

Data depicted on this map include a generalized geologic background and minerals distribution according to the main metal or mineral content, type, age, and size of each individual deposit. Compilation was made from many published and unpublished national geologic and metallogenic maps at various scales. The data were plotted first at 1:1,000,000 scale, then transferred to 1:5,000,000 scale, and finally to 1:10,000,000 scale. This required considerable simplification, especially for the Central Andes, which contain the largest proportion of the mineral deposits; therefore, more small deposits are retained in the less mineralized regions of the Northern and Southern Andes.

Compilation of this map involved work and contributions from many individuals and organizations. Philip W. Guild, as adviser to the Mineral-Resources Map series since the inception of the Map Project, took the lead in the selection of map elements, units, and symbology, especially for land resources. David Z. Piper and Theresa R. Swint-Iki were responsible for most of the compilation and analysis of seafloor mineral data.

All the panel members of the Southeast Quadrant became deeply involved in the compilation of this map and not only contributed expertise, but also, after consulting with their colleagues in their own countries, provided abundant data and advice. They also prepared special maps and summary reports to contribute to the Project. Information from the Northeast Quadrant Mineral-Resources Map (Drummond, 1985) was used for the overlap area with the Northeast Quadrant. Others who contributed substantially are identified on the map. We have attempted to acknowledge all the data sources used and apologize for any inadvertent omissions. The Mineral-Resources Map of the Southeast Quadrant was prepared under the general direction of Panel Chair José Corvalán D., Servicio Nacional de Geología y Minería, Santiago, Chile, with the coordination of General Chair George Gryc and the technical advice of Warren O. Addicott and Theresa R. Swint-Iki, U. S. Geological Survey, Menlo Park, California. Cartographic work was carried out by Frank J. Sidlauskas, Jr., U.S. Geological Survey, Reston, Virginia.

The following Southeast Quadrant panel members contributed directly to the compilation of this map: José Corvalán D., Chair, Chile; Marcelo R. Yrigoyen, Argentina; Anibal Gajardo, Chile; Joaquín Buenaventura and Hermann Duque-Caro, Colombia; Giovanni Rosania and Horacio Rueda, Ecuador; Victor R. Eyzaguirre, Peru; and Alirio Bellizzia and Nelly

Pimentel, Venezuela. Important written contributions to the present text were provided by Alirio Bellizzia, Nelly Pimentel, and Joaquín Buenaventura.

RESOURCE SYMBOLS

Because mineral resources vary widely in their characteristics, the symbols that represent the deposits have been designed to impart as much information as possible at the map scale. Although the map explanations give the details, a brief discussion may be helpful to the reader.

LAND RESOURCES

The legend for the land mineral resources has been modified and simplified from that used for the Preliminary Metallogenic Map of North America (North American Metallogenic Map Committee, 1981) and described by Guild (1981). The map symbols show the metal or mineral content of the deposits by colored geometric shapes. The colors, insofar as possible, group metals or minerals of similar type: for example, copper and associated metals are orange, precious metals are yellow, and lead-zinc and associated minerals are blue. The 5 shapes and 10 colors indicated on the legend of the map provide for 50 combinations.

Three symbol sizes denote the relative importance of the deposits. Limits between the size categories for each commodity are, for the most part, in terms of metric tons of the substance(s) contained before exploitation. These limits are arbitrary and have been selected on the basis of the worldwide abundance of the commodity concerned in deposits that are exploitable under current economic and technological conditions.

Some deposits shown as small on this map correspond to occurrences; they have been included because they may help to identify areas broadly favorable to exploration planning for specific minerals.

One difference from the Northeast Quadrant Mineral-Resources Map should be noted; the age of mineralization categories have been changed for this quadrant.

One or more ticks on the symbol indicate the general nature of the deposit—for example, vein, stratabound, laterite, and placer. Most of the eight deposit types are distinctive, but the category designated "stockworks, including 'porphyry' deposits" encompasses such disparate types as sulfur in the cap rock of salt domes, manto deposits, and porphyry deposits, so judgement must be used in interpreting this symbol. The ticks have been omitted on many of the small symbols either because of ignorance of deposit type or because it was felt unnecessary to identify all of them where they occur in clusters of deposits of the same kind. A description of the eight deposit types shown on the Southeast Quadrant follows:

Veins and shear-zone fillings. Crosscutting, epigenetic deposits in any type of host rock. The major dimensions are transverse to stratification in sedimentary or volcanic hosts. Most stockworks fit here; some in igneous hosts are better equated with the irregular disseminated deposits.

Stratabound, including magmatic cumulates. Deposits, generally of limited horizontal extent, that occur at more or less the same horizon in stratified rocks. May be partly concordant, partly discordant with enclosing rocks. Usually considered to be epigenetic. Examples: carbonate-hosted (Mississippi Valley) base-metal deposits, uranium deposits of Colorado Plateau, Wyoming Basin, and so forth. Magmatic cumulates are concordant in layered, generally mafic or ultramafic igneous rocks. Examples: stratiform chromite, ilmenite, platinum-group metals of Bushveld type; certain nickel sulfide (komatiite-hosted) deposits.

Stockworks, including "porphyry" deposits. Irregular disseminated deposits, in or associated with intrusive igneous rocks. Parts of some have been described as stockworks. Hydrothermal alteration, including greisenization, common.

Magmatic and irregular massive deposits; includes pegmatites. Examples: podiform chromite, some magnetite and magnetite-ilmenite deposits.

Skarn or greisen deposits. Contact-metamorphic (tactite) deposits. Stratified, usually carbonate, rocks intruded by intermediate to acid igneous rock.

Sandstone (red bed) deposits.

Laterite deposits (surficial chemical concentrations). Includes laterite, bauxite, uraniferous calcrete, and some manganese oxide deposits. The criterion is that supergene processes were responsible for producing ore-grade material.

Placer deposits (surficial mechanical concentrations). Includes "fossil" black sands.

Mineralization ages for some deposits are indicated by double ticks placed in clockwise order from older to younger. Where a tick indicating deposit type already occurs, a single tick for age is added and the two must be read together.

Space limitations do not permit identifying by name all the deposits shown on the map, but many of the larger ones are named.

SEAFLOOR RESOURCES

The potential value of manganese nodules depends on their abundance and composition. Abundance data have been derived principally from seafloor photographs, typical examples of which are reproduced in the explanation on the map. Nodules cover from 0 to nearly 100 percent of the seafloor areas. On the map, squares 2 mm on a side, empty to totally filled in black, indicate where bottom photographs have been taken and the abundance of nodules at these points. Additional

information on the occurrence of nodules was gained from core sampling; small black x's and o's indicate where nodules have been recovered or not recovered, respectively, in cores. Details of the methods used in studying these data sources and in deriving abundance contours are described later.

The composition of analyzed nodules is indicated within certain limits by different colored +'s for ranges of nickel plus copper content and by brown +'s with chemical symbols for those with high manganese or high cobalt. Areas of nodules averaging 1.8 percent or more nickel plus copper (considered as potentially exploitable—McKelvey and others, 1979) are outlined in red.

The polymetallic sulfide deposits thus far discovered on the spreading ridges are shown by black semicircles and identified with a name and, for most, a latitude. Occurrences of sulfides, found in Deep Sea Drilling Project (DSDP) and Ocean Drilling Program (ODP) cores, which may have originated at a ridge and moved off it since their formation, are shown by smaller semicircles and identified by the DSDP or ODP site number.

Submarine hot springs not related to seafloor spreading, which in a few nearshore locations are known to be precipitating metallic minerals (though not in economic quantities), are shown by open semicircles.

Seafloor phosphorite occurrences are depicted by brown horizontal lozenges without an outline. Although this symbol is approximately as large as that used for the medium-sized land deposit, it has no size or grade significance.

LAND RESOURCES

By
José Corvalán D.

GEOLOGIC SETTING

The most important geologic features in relation to mineral deposits of the Southeast Quadrant of the Circum-Pacific Map Project are the Andean Cordillera and the Caribbean Mountain System, which form the Pacific and northwest margins of the South American continent, respectively. Other important geologic features of the quadrant are parts of two shield areas, the Guyana and Brazilian, consolidated at the end of the Precambrian, and extensive regions of largely undeformed and thick sequences of sedimentary and volcanic rocks that constitute platform cover over the Precambrian basement of the South American Platform, and over the middle Paleozoic basement of the Patagonian Platform, the latter located entirely within Argentina.

The main mineral resources of the Southeast Quadrant are directly related to the geotectonic evolution of the Pacific continental margin of South America, with the most important ore deposits emplaced during a time of tectonic segmentation during the Mesozoic and Cenozoic Eras. This segmentation controlled successive episodes of sedimentary accumulation and extrusive and intrusive magmatism and deformation that occurred at the convergent plate edge. The evolution of the three main segments–the Northern, Central, and Southern Andes–varied, causing the different nature and geologic environments of the mineral resources now found in each segment, and defining the unique character of this region.

There is evidence of accretionary processes along the entire length of the west margin of South America during the Paleozoic, but such processes were apparently absent during the Mesozoic and Cenozoic in the Central Andes, where they were replaced by active subduction-erosion and intense and widespread magmatism.

Mineral distribution in the Central Andes, limited by the tectonic boundaries of the Huancabamba Deflection at the north and the Bariloche Transversal at the south, forms elongate subparallel belts that correspond to metallogenic provinces or subprovinces. These are not clearly distinguished in the Northern and Southern Andes.

Although very simplified, the geologic background used on this map, taken from the Southeast Quadrant Geologic Map (Corvalán, 1985b), depicts the difference between these three main segments of the Andes. A main difference from the geologic map is that some of the geologic units used on the mineral-resources map denote structural state (unfolded, deformed, or strongly metamorphosed) and depositional environment of the stratified rocks rather than geologic age; igneous rocks are differentiated by color and pattern. Letter symbols keyed to the correlation diagram indicate ages of rock in most areas. The main morphostructural limits of the Andean region and nomenclature used in this report are shown in fig. 1. The following units are discussed by age from older to younger, emphasizing their economic importance.

GEOLOGIC UNITS

Precambrian crystalline rocks

The Precambrian crystalline rocks include the undivided Precambrian rocks which constitute the large areas of the Guyana and Brazilian Shields; metamorphic rock, migmatite, and anatectic granite of southeastern Colombia, possibly extending into the Eastern Cordillera of Ecuador and north-central Peru; schist, gneiss, and amphibolite in the Sierra de Perijá; metamorphic rocks and associated granitoids of the Pampean Ranges and Patagonia Massif; and smaller areas of outcrops, mainly in the coastal ranges of southern Peru (Arequipa Massif) (fig. 1).

Mineral deposits occur mainly in the shield areas with large deposits of iron, gold, and extensive

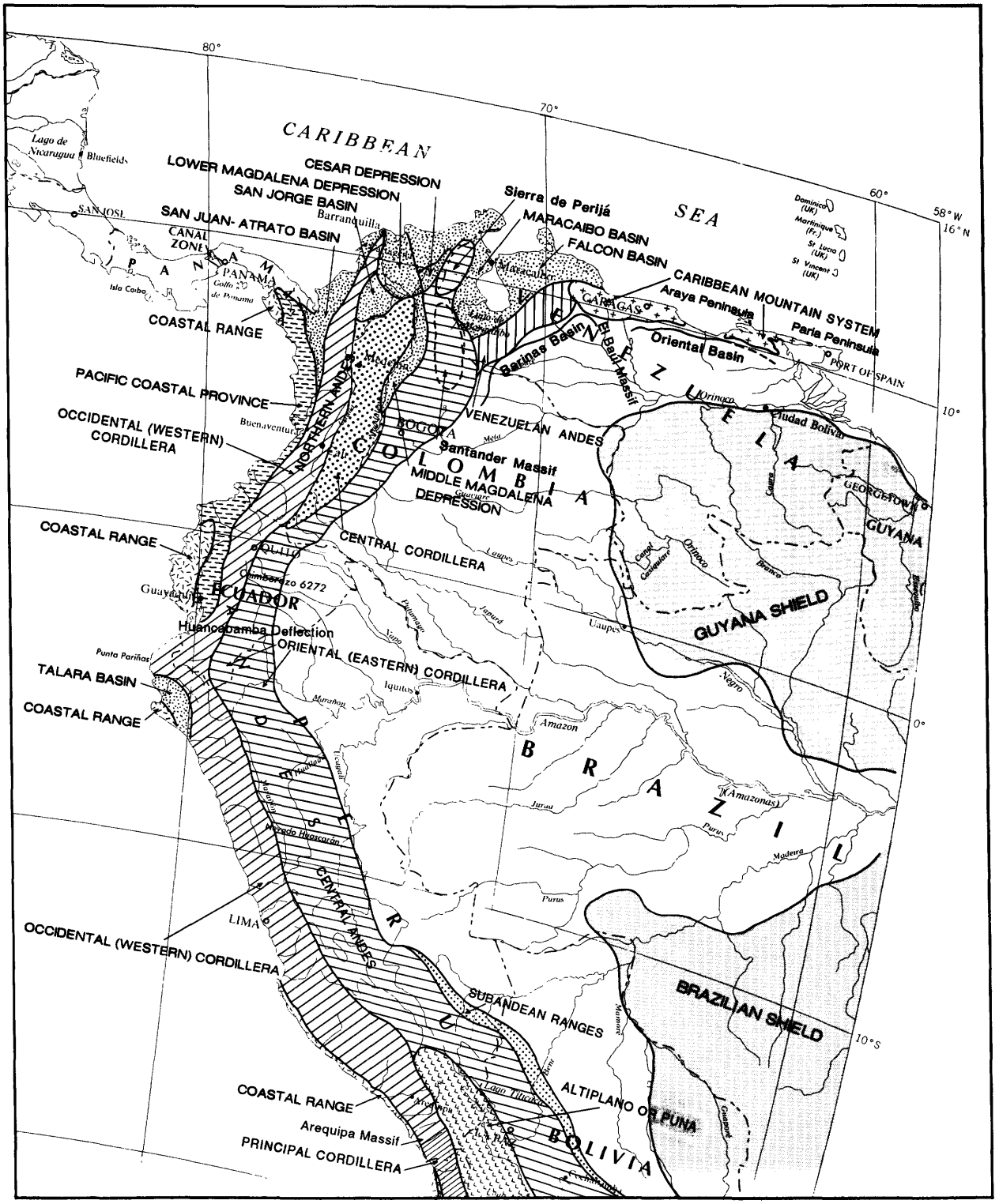

Figure 1*A*. Principal morphostructural features of the Andean Belt, adapted from Auboin and others (1973) and Corvalán (1979). *A*, northern South America and Central America.

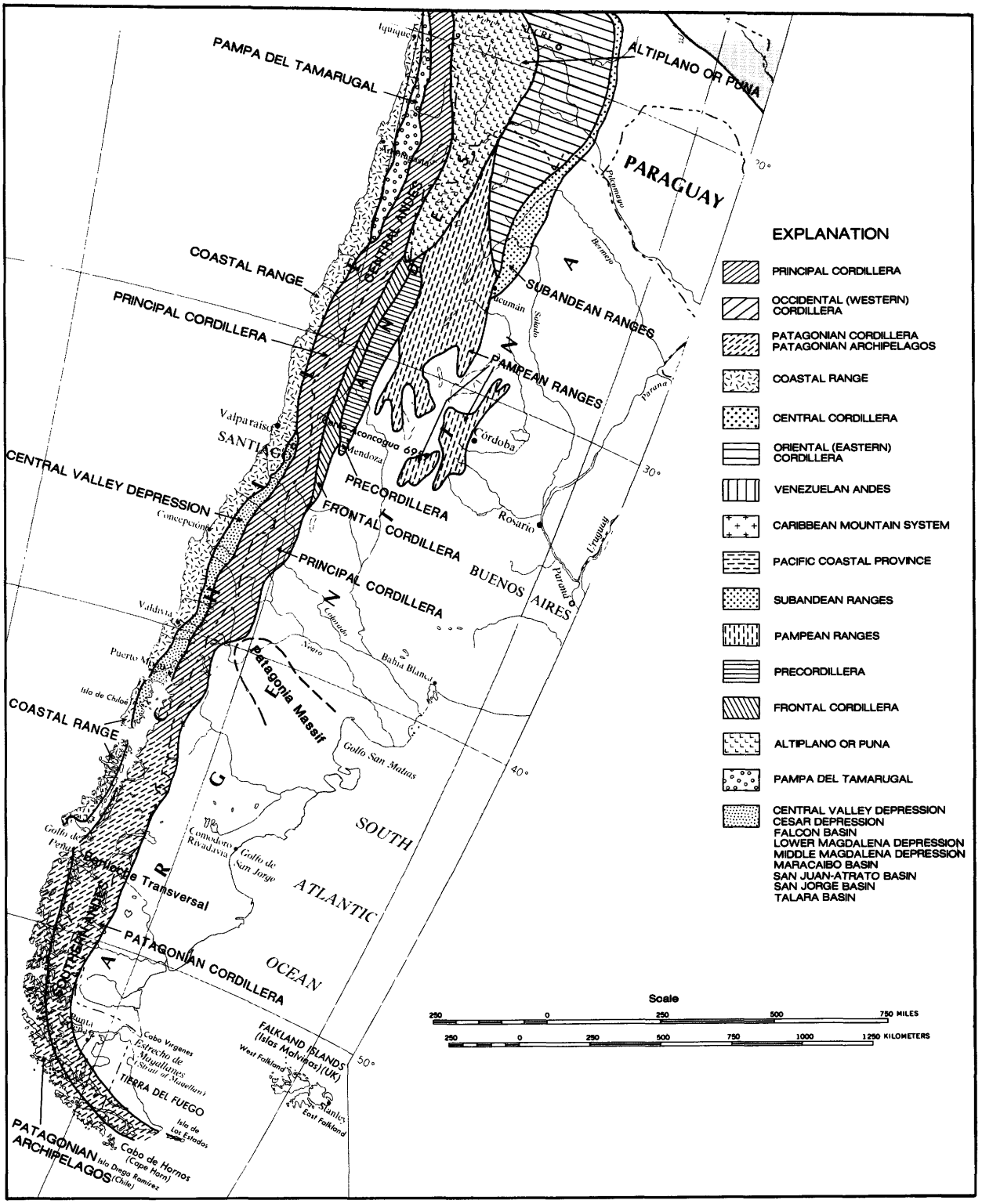

Figure 1*B*. Principal morphostructural features of the Andean Belt, adapted from Auboin and others (1973) and Corvalán (1979). *B*, southern South America.

aluminum (bauxite) such as those at Los Guaicas, Kamoirán, and Nuria, along with laterite in the Guyana Shield. Iron is related to the granulitic belts of the Imataca Complex (early Precambrian); important deposits are Cerro Bolívar and El Pao. Important vein-type gold deposits in the Venezuelan Guyana Shield are the mining districts of El Callao, Botanamo, and Vuelvan Caras. The most favorable host rocks are meta-andesite and metabasalt with advanced propylitization. Placer gold deposits are also abundant in this geologic environment and have provided the largest gold production in Venezuela. Numerous small to medium placer tin deposits also occur in the shield areas.

In Colombia, there are some occurrences of uranium, copper, and base-metal mineralization but none are economically important. Tungsten, beryllium, chromium, and uranium deposits are known in the Precambrian rocks of the Pampean Ranges of Argentina.

Metamorphic complexes of Phanerozoic age

Metamorphic rocks of Phanerozoic age, mostly early Paleozoic and Mesozoic, constitute the host rocks of several small vein-type copper and gold deposits in Venezuela, as well as copper, gold, silver, manganese, and iron in Colombia and the coastal ranges of Chile, with itabirite-type iron deposits in the latter. Except for these large but low-grade banded iron deposits, most are of no economic importance.

In the Venezuelan Andes the most important copper deposits are the volcanogenic massive sulfides found near the border between the states of Táchira and Mérida (Rodriguez, 1990). They consist, as in the Bailadores deposit, of masses of copper-lead-zinc sulfides emplaced in a thick sequence of metavolcanic and metasedimentary rocks of Paleozoic age. Other copper deposits in Venezuela are associated with Mesozoic metavolcanic and metasedimentary rocks (Aroa Formation) of the Caribbean Mountain System (such as the Aroa, San Antonio, and Sanjón Verde deposits).

The large nickel deposit, Loma de Hierro, associated with peridotite of the ophiolitic Loma de Hierro Complex, includes gabbro, volcanic breccia, pillow basalt, and thin intercalations of tuff, limestone, and radiolarian-bearing lutite of Early Cretaceous age. The deposit is a typical nickeliferous laterite resulting from the weathering of peridotite and serpentinite.

The itabirite-type iron deposits of Chile are in metamorphic rocks of the "metamorphic basement" of the Coastal Range, with a minimum age of Carboniferous (~340 Ma).

Ultramafic rocks

Peridotite or its hydrous altered variety serpentinite and/or associated ophiolitic complexes occur at several regions in the Southeast Quadrant. Economically important are those of Venezuela, Colombia, and Ecuador for their potential for chromite and nickel deposits.

In the Caribbean Mountain System the large nickel deposit Loma de Hierro derives from the chemical weathering of peritodite (serpentinized harzburgite) associated with gabbro, volcanic breccia, and pillow basalt, with thin intercalations of tuff, lutite, and radiolarite of Early Cretaceous age. The zoned ultramafic complex of Tausabana-El Rodeo of the Paraguaná Peninsula in Venezuela, composed of dunite, harzburgite, and hierzolite, bears some chromite mineralization.

The Cretaceous sequences exposed west of the Romeral Fault System in Colombia include the Diabasic Group (Julivert, 1973) consisting of basic volcanic rocks which, according to their chemical characteristics, correspond to oceanic crust (Aguirre, 1989). Several ultramafic bodies are known to occur along the Romeral Fault System, where the large Cerromatoso nickel deposit is located. A similar geologic environment is recognized in Ecuador west of the Guayaquil Suture, where the Basic Igneous Complex (Goossens and Rose, 1973) and the Piñon Formation (Baldock, 1982) include ultramafic and mafic rocks of oceanic affinities.

In Central America (Costa Rica and western Panama) the Nicoya Complex possibly corresponds to the Basio Igneous Complex of Ecuador and equivalents in Colombia. Its lower part is an ophiolitic association of gabbro, dolerite, and massive and pillow basalt (olivine tholeite), whose geochemical character indicates that it represents oceanic crust (Gursky and others, 1985).

Some occurrences of serpentinized peridotite have been reported from the Paleozoic Metamorphic Basement (Western Facies) of southern Chile (Hervé, 1977) in which some minor chromite mineralization exists. Also, in southern Chile, an ophiolitic association of gabbro and pillow basalt of Late Jurassic-Early Cretaceous age (Tortuga Complex, Suárez, 1977) is known to have been emplaced on the continental margin of the Patagonian Cordillera.

Unmetamorphosed sedimentary and volcanic rocks of Paleozoic age

Grouped under this unit are unmetamorphosed to weakly metamorphosed sedimentary rocks (mostly marine, but also continental, glacial, and marine-glacial) and volcanic rocks predominantly of silicic composition.

Marine sedimentary rocks range in age from Cambrian to Carboniferous and Early Permian, and constitute an extensive Paleozoic cover in the Eastern Cordillera of Peru and Bolivia, in the Sub-Andean ranges of Bolivia, and in northwestern Argentina. In Peru and Bolivia the early Paleozoic sequences (Cambrian to Devonian) locally contain conglomerate and ferruginous sandstone. The marine sedimentary rocks are generally

overlain by continental clastic, plant-bearing sedimentary rocks, and by extensive, predominantly silicic volcanic rocks of Late Permian and Early Triassic ages.

Many ore deposits lie in this geologic environment, but in many cases the age of their formation is post-Paleozoic, as with the tin deposits of Bolivia, formerly thought to be Silurian, now considered to be genetically related to intrusive rocks of Late Triassic to late Tertiary age (Urquidi-Barrau, 1990).

The large lead-zinc deposit of Sierra Aguilar in northwestern Argentina has been interpreted as a stratabound sedimentary-diagenetic deposit of Silurian age (Sureda and Amstutz, 1981). In the same general area and of the same age are various medium-sized stratabound iron deposits that occur in the Sierra de Zapala and Santa Bárbara. In addition to the probably syngenetic large Cobriza copper deposit of Peru emplaced in late Paleozoic limestone (Husman and others, 1987), several small to medium deposits of lead-zinc, copper, nickel, chromite, gold, and large tungsten deposits are emplaced in this Paleozoic belt, mostly in Peru, Bolivia, and Argentina.

Arc-backarc sequences

This unit includes all of the stratified Mesozoic and early Cenozoic formations that constitute the Central Andes. Throughout its longitudinal extent, this belt includes the most important and numerous mineral deposits of the Andean region, in most cases genetically related to extrusive and intrusive magmatism. Volcanogenic, syngenetic, epigenetic, and continental stratabound deposits, veins, stockworks including porphyry deposits, magmatic, irregular, and skarn deposits are all common in this environment. It is characterized by an active and persistent volcanism generated at several migrating magmatic arcs, and by filling of backarc basins during a changing paleogeography. In the southern part of the Central Andes (Chile and Argentina), the stratified units register accumulation around an oceanic magmatic arc, predominantly in marine backarc basins, from the Late Triassic to the Early Cretaceous, and around a continental magmatic arc, in intermontane basins, from the Late Cretaceous to the early Cenozoic.

By contrast, in the northern part of the Central Andes (Peru and Bolivia), the volcanogenic and sedimentary marine sequences also began to accumulate in the Late Triassic, but they are as young as Late Cretaceous; only the stratified rocks of early Cenozoic age are of continental volcanic and sedimentary origin. This differing evolution may account for the varying types of mineralization in these two segments. Intrusive magmatism and several phases of compressional deformation affected the rocks accumulated mainly in the Late Jurassic, Late Cretaceous, and early Tertiary, during the most important orogenic diastrophism of the Andean orogenic cycle. Mineralization occurred at different times during the evolution of this paleogeographic environment.

In the Coastal Ranges of central and northern Chile and central Peru, numerous medium to large iron deposits are emplaced mostly in the volcanogenic and continental-clastic sedimentary formations of Jurassic and Early Cretaceous age. These iron deposits are stratabound, such as Almaden and Monterrosas in Peru; vein-type, which are very abundant; and magmatic and irregular massive deposits like Algarrobo, El Tofo, and Romeral in Chile. These last deposits consist of magnetite, hematite (specularite), and apatite, formed by replacement and contact metamorphism in andesitic lava of Neocomian age. These iron deposits, together with stratabound syngenetic sedimentary-volcanic manganese deposits, also of Early Cretaceous age, form a well-defined iron-manganese belt in Chile (Ruiz and Lowell, 1990). Copper, molybdenum, gold, and silver are the most important mineral resources in this geologic environment, as is significant mineralization of lead and zinc in central Peru (such as the Morocha, Quiruvilca, Cerro de Pasco, and Hualgayoc deposits).

Medium and large silver and gold deposits occur especially in Chile and Peru, generally east of the iron-manganese belt. Deposits hosted in Jurassic and predominantly Cretaceous rocks form a western belt of gold and silver mineralization in Chile (for example, the Huantajaya, Chañarcillo, Caracoles, El Guanaco, and El Chivato deposits). Recently, however, large new deposits have been found in an eastern belt typified by the Indio Mine, and hosted in a different geologic environment of Cenozoic volcanism, discussed later in this text.

Emplaced in host rocks of as young as late Cenozoic age is the most important copper mineralization in the Central Andes; the large, high-grade porphyry copper deposits of central and northern Chile and southern Peru are genetically related to diorite to quartz monzonite porphyry stocks, which form subbelts radiometrically dated as Paleocene and early Eocene (65 to 51 Ma), late Eocene and early Oligocene (41 to 31 Ma), and middle and late Miocene (16 to 5 Ma) (Sillitoe, 1990). Mineralization occurs in stockworks or in breccia pipes exhibiting zonal hydrothermal alteration and sulfide mineralization. The main porphyry copper deposits in Peru are La Granja, Michiquillay, Pashpap, Cerro Verde, Cuajone, Quellaveco, and Toquepala; in Chile, Cerro Colorado, Quebrada Blanca, Chuquicamata, El Abra, La Escondida, El Salvador, Potrerillos, Los Palambres, Rio Blanco, Disputada, and El Teniente. In Argentina, the El Pachón and Bajo de la Lumbrera deposits are included in the middle and late Miocene subbelt of mineralization (Sillitoe, 1990).

Forearc, island-arc, and marginal-basin sequences

The geologic and structural characteristics of the Mesozoic and early Cenozoic deposits of the Northern and Southern Andes differ strongly from the chronologically equivalent formations of the Central Andes. This is mainly expressed in the inclusion of oceanic crust and associated deep-water flysh-type marine sediment in the Jurassic and Cretaceous sequences and in a structural development characterized by compressional tectonics that created complex overthrusts and reverse-fault systems. This geologic evolution, which included accretionary processes at the end of the Cretaceous in the Northern Andes, was probably the main factor causing mineralization different from that of the Central Andes.

Forearc associations are found along the coastal region of Ecuador (Basic Igneous Complex, Goossens and Rose, 1973), which include basaltic lava, diabase, and mafic intrusive rocks of Late Jurassic to Early Cretaceous age, and on the Western Cordillera (Formación Diabásica-Porfirítica, Sauer, 1965), where a mafic to ultramafic unit contains intercalated nonfossiliferous lutite and silicic sedimentary rocks. Late Cretaceous forearc associations are found in western Ecuador, consisting of basaltic breccia, flows, and pillows, with tholeitic affinities, and interbedded turbiditic volcaniclastic sedimentary rocks and thin bedded pelagic sedimentary rocks (Piñón Formation, Baldock, 1982; Cayo Formation, Olsson, 1942). A similar stratigraphic sequence is found in Colombia, in parts of the Cordillera Occidental and western part of the Cordillera Central (Diabasic Group, Julivert, 1973).

In this geologic environment, the most important mineral deposits are those of nickel, the largest being Cerromatoso in Colombia, which consists of nickeliferous laterite derived from weathering of Cretaceous ultramafic rocks along the Romeral Fault System.

Loma de Hierro, in the Caribbean Mountain System, is another important nickeliferous laterite deposit derived from weathering of peridotite and serpentinite of the Early Cretaceous ophiolitic Loma de Hierro Complex.

Chronologically equivalent backarc deposits in Colombia, Venezuela, and Ecuador are volcanic-free marine sedimentary rocks, which contain several economically important intercalations of phosphorite deposits.

In the Southern Andes, aside from a few small intrusive-related copper deposits, known mineralization is scarce. The Early Cretaceous lithologic assemblages are interpreted as island-arc and marginal-basin, with ophiolitic associations and shelf accumulations (Suarez and Pettigrew, 1976). The Late Cretaceous marine sedimentary rocks of this region contain abundant molasse and flysh deposits (Cecioni, 1957).

Basinal and marginal deposits

Marine and continental sedimentary rocks, mostly of Neogene age, accumulated in successor basins developed by localized subsidence after the major Andean compressional deformation was completed. Shallow-water marine sedimentary rocks containing phosphorite deposits predominate along the Pacific margin. Interior basins contain continental deposits, some of which include important coal resources.

Undeformed extrusive volcanic rocks

Grouped under this unit are continental volcanic rocks and intercalated sedimentary rocks, which constitute an extensive flat-lying or tilted and faulted cover of Neogene and Quaternary age, unconformably overlying the Paleogene and older formations. The composition of the volcanic rocks ranges from felsic (rhyolite) to mafic (basalt). This cover includes all recent and older (Quaternary-late Tertiary) volcanic centers and associated structures (calderas, domes).

Extensive areas of Central America are covered by Tertiary intermediate to mafic and Quaternary mafic volcanic rocks.

In the Andean region, intermediate to mafic volcanic rocks, mostly of Quaternary age, form a continuous belt extending from southern Colombia into Ecuador.

The most extensive volcanic cover is found as an almost continuous unit from southern Peru into western Bolivia, northwestern Argentina, and northern Chile, forming the Altiplano Region. The average thickness of this unit is about 1,000 m; the volcanic rocks are mostly rhyolitic to dacitic ignimbrite with subordinate andesite. Locally, basalt is found at the more recent volcanic centers. In the eastern part of the Antofagasta region in northern Chile, the volcanic cover includes the unique high-grade iron deposit El Laco, constituted almost entirely of magnetite and subordinate hematite. South of parallel 33°S, the volcanic cover is mostly of andesitic to andesitic-basaltic composition.

Recent studies (Tavera and others, 1993) have shown the economic importance of the Neogene and Quaternary volcanic cover, especially in northern Chile, southern Peru, and southwestern Bolivia, where many volcanic centers, including calderas, stratovolcanoes, and dome complexes host epithermal precious-metal deposits.

Surficial deposits

Large areas on the map depicted as Quaternary correspond mostly to surficial deposits of various types; other occurrences are too small to be represented at this scale. The most common mineral resources in this environment are placer deposits of heavy minerals such

as gold, platinum, chromite, cassiterite, magnetite, and ilmenite, derived from older rocks. Gold placer deposits in the Southeast Quadrant are segregated by fluvial or fluvioglacial processes or by wave action on beaches. Platinum placers are rare but are known in the region of Chocó in western Colombia.

Other important mineral deposits, the result of different geologic and geographic conditions, are contained in brine and evaporite. The Central Andes, mainly in Bolivia, Chile, and Argentina, contain many salars, former lakes in areas of internal drainage and under progressive desiccation, in which elements leached from the country rocks have concentrated. The largest proven economically important concentrations of lithium, potash, and sodium have been found in the salars of Atacama (Chile), Uyuni (Bolivia), and Hombre Muerto (Argentina) (Ericksen and Salas, 1990; Ide and Kunasz, 1990).

Intrusive igneous rocks of Phanerozoic age

Intrusive igneous rocks of Phanerozoic age are widespread in the Southeast Quadrant, forming extensive batholiths ranging in age from Paleozoic to early Tertiary; younger intrusive stocks are geographically restricted.

Many of the mineral deposits of the Southeast Quadrant are demonstrably related to the intrusive rocks. These include porphyry deposits, skarns, magmatic segregations, and vein deposits. But because of the small scale of the map, no attempt was made to represent them separately. Information on the intrusive rocks should be taken from the Southeast Quadrant Geologic Map (Corvalán, 1985b).

The composition of the intrusive rocks ranges mostly from felsic to intermediate; in places, although not commonly, individual plutons show local variation to mafic extremes. In the Andean region of Chile and Argentina, batholith emplacement ages decrease toward the east. An extensive Paleozoic (mostly Carboniferous) batholith in the coastal region of Chile is followed eastward by radiometrically dated Jurassic, Cretaceous, and Tertiary batholiths, the last emplaced in the main Cordillera (Aguirre and others, 1974). These migrating intrusive belts are spatially related to corresponding eastward-migrating volcanic arcs, fundamental to mineral exploration.

PRINCIPAL MINERAL DEPOSITS

As a complement to the Southeast Quadrant Mineral-Resources Map, the following is a summary of the most important minerals and types of deposits in the region. No attempt is made to discuss metallogenic provinces or subprovinces, not depicted on the map, inasmuch as these have been the subject of various authors (Ericksen, 1976, 1980; Ruiz and Ericksen, 1962; Ruiz and others, 1965; Sillitoe, 1976, 1988, 1990).

Only the principal ore deposits are shown, to indicate their relative importance, type, and, not always possible to show adequately on such a small-scale map, most common geologic environment. Except for cases where information was readily available, mineralogy and reserves of the deposits have not been included; the latter information can, in a general way, be deduced from the map's explanation. Compilation was made from the most important and comprehensive publications on Andean ore deposits and from unpublished information provided by the Southeast Quadrant panel members.

Copper

Copper is by far the most common and most important economic mineral resource in the Southeast Quadrant region. Although copper mineralization is known to occur throughout the entire length of the Andes, Chile and Peru have the world's largest and highest grade copper deposits. Copper in the Andes has been estimated to account for about 40 percent of world copper resources (Sillitoe, 1990). It occurs in several types of deposits, the most important and widespread being porphyry, manto, skarn, and vein deposits (figs. 2, 3).

Porphyry copper

The most prominent mineral-resource feature in the Andean region is the long and continous porphyry copper belt extending from central Chile to Peru and southern Ecuador. Along this belt, Chuquicamata and El Teniente are the largest deposits; also very important are El Abra, Quebrada Blanca, Collahuasi, and Cerro Colorado in the north, and La Escondida, El Salvador, Potrerillos, Los Palambres, Rio Blanco, Los Bronces (Chile), and El Pachón (Argentina) in the south. Intrusive rocks related to these deposits are generally of late Eocene and early Oligocene age, except for Río Blanco, Los Bronces, El Teniente, and El Pachón (Chile), which are middle and late Miocene, and Cerro Colorado (Chile), which is Paleocene to early Oligocene (Sillitoe, 1990). Andacollo (Chile) is an important deposit within a poorly defined Cretaceous subbelt. In central Argentina, the porphyry copper deposits of Paramillos Norte, Paramillos Sur, and Campana Mahuída are associated with Cretaceous intrusive rocks.

This porphyry copper belt extends into southern Peru, where the important deposits of Toquepala, Quellaveco, Cuajone, and Cerro Verde-Santa Rosa are located. There, the intrusive rocks related to these deposits are of Paleocene and early Eocene age. To the north in Peru and beyond to southern Ecuador, porphyry copper deposits such as Toro Mocho, Pashpap, Michiquillay, La Granja, Cañariaco, and Chaucha

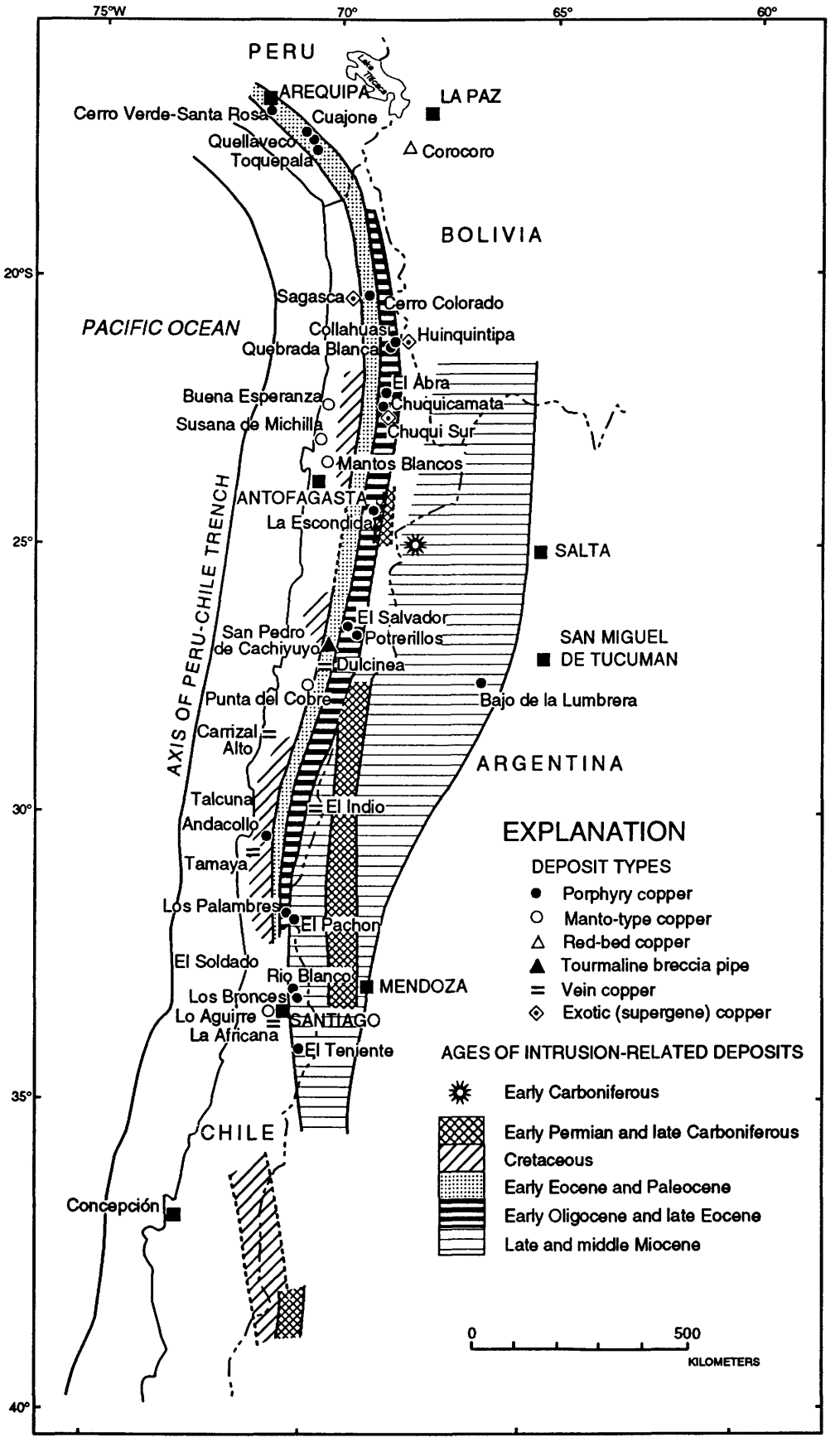

Figure 2. Major copper deposits in the Andes of Chile, Bolivia, and Argentina. Ages of subbelts for intrusion-related deposits (taken from Sillitoe, 1988).

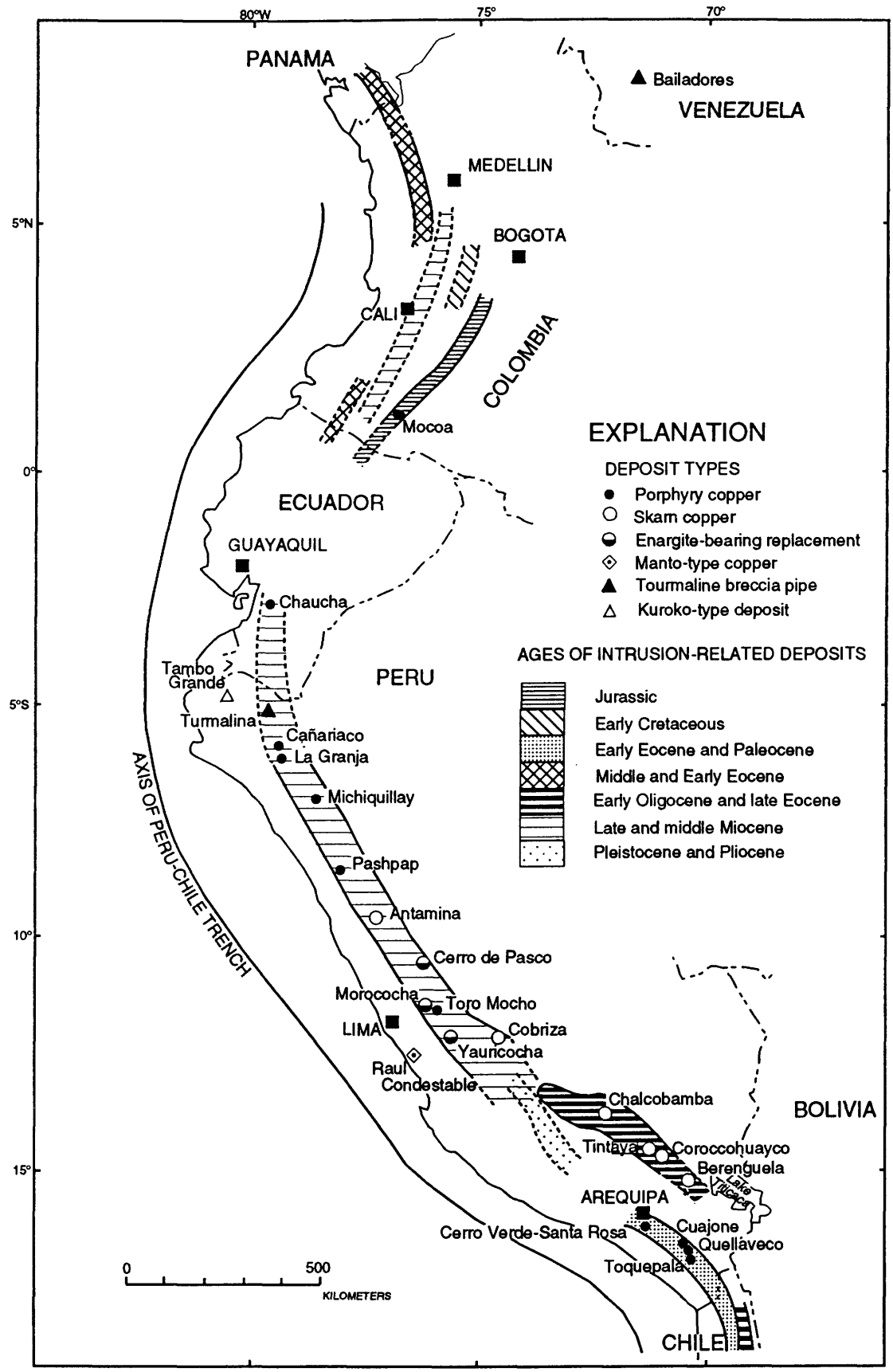

Figure 3. Major copper deposits in the Andes of Colombia, Ecuador, and Peru. Ages of subbelts for intrusion-related deposits (taken from Sillitoe, 1988).

(Ecuador) are within a belt of associated middle and late Miocene intrusive rocks. The copper-molybdenum deposit of Chaucha is within the copper subprovince of the Cordillera Occidental of Ecuador, associated with moderately silicic hypabyssal intrusive rocks (Paladines and San Martín, 1980); other prospects have been located in the same geological environment in southern Ecuador. In Colombia, the copper-molybdenum Mocoa deposit is the most important and is associated with Jurassic intrusive rocks; the highest grades of copper and molybdenum here are concentrated in irregularly shaped hydrothermal breccia in both potassic and sericitic alteration zones. Preliminary studies have estimated reserves of 300 million tons of ore with 0.37 percent copper and 0.061 percent molybdenum at the Mocoa deposit. This oceanic deposit formed in a western copper belt in Ecuador; two eastern continental copper belts contain the known prospects of Infiernillo, Chili, Dolores, and California.

In Central America, copper-molybdenum porphyry deposits are known in Panama (Cerro Colorado and Petaquilla).

Skarn copper

The most important skarn copper deposits are in Peru. In southeastern Peru, calcic skarn copper-iron deposits (Coroccohuayco, Tintaya, and Chalcobambo) and copper-silver deposits (Berenguela) occur in the Andahuaylas-Yaurí subbelt of late Eocene and early Oligocene intrusive rocks. In central Peru, the Antamina and Cobriza deposits are within a belt of middle and late Miocene intrusive rocks, but their age of mineralization is uncertain (Sillitoe, 1990).

Minor copper skarn deposits occur in Chile (La Campana, Los Maquis, Panulcillo) and in Colombia (Mina Vieja, El Sapo) (Petersen, 1990). Two types of skarn deposits are known in west-central Argentina; copper is the principal economic metal in the first type (Las Choicas), and iron in the second type (Colipilli and Hierro Indio districts in Mendoza Province).

Other sources of copper are the enargite-bearing replacement copper deposits such as Yauricocha, Morococha, and Cerro de Pasco in Peru (Sillitoe, 1990). Sillitoe suggests that they correspond to a type of mineralization in high-level volcanic to subvolcanic settings, especially in the upper parts of porphyry copper systems.

Manto deposits

Manto-type (or stratabound) copper deposits are abundant in Chile, where they occur in volcanic-sedimentary sequences clearly related to magmatic arcs, and accumulated during the Jurassic, Early Cretaceous, Late Cretaceous and even early Tertiary in various parts of the country (Ruiz and others, 1965). They consist chiefly of chalcopyrite, bornite, pyrite, and lesser amounts of primary chalcocite, covellite, and specularite. Many of them are stratiform; others are irregular bodies, limited to a specific stratigraphic unit of either volcanic or sedimentary rock (Ruiz, 1990). In northern Chile these deposits are mainly hosted in Jurassic volcanic rocks of the Coastal Range (Buena Esperanza, Michilla, Mantos Blancos). Numerous manto-type copper deposits are emplaced in volcanic-sedimentary rocks of Early Cretaceous age (Punta del Cobre, Talcuna, Guayacán, El Soldado, Lo Aguirre); others, like Cerro Negro, are in Late Cretaceous sequences and less commonly in rocks as young as Late Cretaceous to Eocene.

The most common host rocks of these deposits are andesitic flows and pyroclastic rocks. In many of the lava deposits, the copper minerals are found in the upper amygdaloidal part of the flow, filling vesicles and small fractures, as well as in disseminated grains in the more aphanitic parts of the flow.

Manto-type copper deposits also occur in west central Argentina within magmatic-arc environments with characteristics very similar to those of central Chile. They contain copper minerals as vesicle fillings in lava and as crosscutting veins in interbedded lava and red beds of Late Jurassic age (Tordillo Formation) (Mendez and Zappettini, 1990).

Raúl and Condestable are the most important manto-type copper deposits in Peru, in the central coastal region; they consist of a series of stratabound lenses in andesitic volcanic and sedimentary rocks of Early Cretaceous age, a geologic environment similar to that of the Chilean manto-type copper deposits. Several occurrences of copper deposits associated with continental sedimentary and volcanic rocks of Jurassic and Cretaceous age (La Quinta Formation) are known in the Sierra de Perijá (Caño Tigre) and the Andean Cordillera (Seboruco and Cerro Mono) in Venezuela. These consist chiefly of chalcocite, chalcopyrite, and pyrite impregnations in sandstone and conglomerate (Rodriguez, 1990).

The most important stratabound copper deposit in Venezuela is that of Aroa in the Caribbean Mountain System. This is associated with a Mesozoic metavolcanic-metasedimentary sequence (Aroa Formation) of phyllite, crystalline limestone, greenschist, and metabasite. Massive lenses parallel to foliation planes contain pyrite, chalcopyrite, and subordinate amounts of sphalerite, galena, covellite, and bornite.

Red-bed copper

The most important red-bed copper deposit is at Corocoro in the Altiplano of Bolivia. The red-bed copper mineralization is hosted by a Tertiary molassic sequence accumulated in an ensialic backarc basin (Sillitoe, 1990).

Kuroko deposits

The most important copper-bearing deposits interpreted as Kuroko-type in this quadrant are those of Tambo Grande in northern Peru and Bailadores in the Andes of Venezuela (Mérida). Tambo Grande is a massive lens of copper-, zinc-, and lead-bearing pyrite in a submarine volcanic sequence of Late Jurassic and Early Cretaceous age. Bailadores is a massive sulfide zinc-lead-silver deposit where a chalcopyrite zone contains copper values ranging from 1.0 to 4.28 percent. Estimated reserves are of 4 million tons of ore (Rodriguez, 1990). The deposit is in a sequence of Paleozoic metavolcanic and metasedimentary rocks.

Vein copper

Copper-bearing vein deposits are most widespread and abundant in central and northern Chile. They were most important during the second half of the 19th century when Chile became the world's principal copper producer. The main mining centers at that time were Tamaya, Carrizal Alto, La Higuera, Brillador, Dulcinea, and Gatico (Ruiz and others, 1965). Other important vein-type copper deposits mined during this century are in the Tocopilla District, the Delirio de Punitaqui and La Africana mines, all of which closed before 1985 (Ruiz, 1990).

Most of these deposits are related to Jurassic to early Cenozoic phaneritic plutons of intermediate composition. Volcanic-hosted copper veins, such as Cerro de Pasco (Peru) and the El Indio gold-silver-copper deposit (Chile), carry enargite as the main copper mineral. At El Indio, ore reserves of 4.7 million metric tons with 5.1 percent copper have been reported (Sillitoe, 1990).

The importance of the vein-type copper deposits has drastically decreased, partly because many of them have been worked out and partly due to the increasing importance of porphyry and manto-type deposits.

Molybdenum

Molybdenum is the main accompanying metal in the porphyry copper deposits of the Andean region. From data compiled by Sillitoe (1990), the highest concentration (0.06 percent) occurs at Mocoa in Colombia; values ranging from 0.035 to 0.052 percent molybdenum are found at Pashpap (0.052 percent) and Antamina (0.04 percent) in Peru, and Chuquicamata (0.035 percent) and Collahuasi (0.04 percent) in northern Chile. Lower grades of 0.02 percent molybdenum occur at Michiquillay in Peru and Quebrada Blanca and Rio Blanco in Chile. Values of 0.013 to 0.014 percent molybdenum occur at Cerro Verde-Santa Rosa, Cuajone, Quellaveco, and Toquepala in southern Peru; in the porphyry copper belt south of La Escondida (Chile), grades of molybdenum range from 0.015 (La Escondida) to 0.018 percent (El Teniente).

Molybdenum also is known to occur in several other ore deposits, where molybdenite in veins or irregular veinlets that contain quartz, tourmaline, and chalcopyrite is associated with granodiorite or altered andesite. Examples of these deposits are Dos Hermanos (Campanani), Copaquire, and Rosario in northern Chile (Ruiz and others, 1965). The Andean and Andean-margin region of southern Chile, especially Aysén, contains minor occurrences of molybdenite. Veinlets of molybdenite are found in granitic rocks at El Portillo and Arroyo Cuevas and in intrusive breccia, not yet exploited, at Polvaredas in west central Argentina (Mendez and Zappettini, 1990).

Iron

Iron deposits and occurrences are widespread in the Southeast Quadrant, but the most important deposits are concentrated in the central Andes, mostly in Chile and Peru, and in the northern Andes, in Venezuela and Colombia. In Chile, a well-defined iron province in the Coastal Range, in which several important iron deposits occur, extends between parallels 26° and 32°S lat, a length of over 600 km. Examples are El Algarrobo, El Tofo, and El Romeral. They are hosted in andesitic lava flows and breccia, usually of Early Cretaceous (mostly Neocomian) age. Mineralization occurs in large massive irregular bodies and consists of magnetite, specularite, and apatite formed by replacement and contact metamorphism in the andesitic lava (Ruiz and others, 1965; Ruiz, 1990). Ruiz (1943, 1961) considers that these deposits originated by contact metamorphism caused by granodioritic intrusions into the volcanic rocks, with magnetite bodies and accompanying minerals formed by metasomatic replacement and fracture fillings. Similar iron deposits in the northern part of this belt are Bandurrias, Adrianitas, and Cerro Imán.

Also in a western iron province, with a similar magmatic-arc environment, are the iron deposits of Marcona in Peru, and Pascuales in southern Ecuador.

Other important but low-grade iron deposits occur in the Coastal Range of southern Chile in the vicinity of Lleu-Lleu Lake (the Relún deposit). These deposits are sedimentary-metamorphic (itabirite-type) (Ruiz and others, 1965) and are included in mica schist of the so-called Metamorphic Basement, originally interpreted as being of Precambrian age, but now known to be no older than Paleozoic (Carboniferous) age. The ferriferous section, about 20 m thick, contains banded iron alternated with silica-rich bands.

A unique high-grade iron deposit, El Laco, occurs in the eastern part of the Antofagasta region in northern Chile (Park, 1961; Ruiz and others, 1965). It consists of five tabular mineralized bodies overlying andesitic lava with strong hydrothermal alteration. The iron bodies are almost entirely constituted of magnetite and hematite.

Their texture and structural characteristics are similar to those of intermediate to basic lava flows, and are associated with andesitic lava of Pleistocene age.

In the Northern Andes, iron deposits of the Precambrian Guyana Shield of Venezuela are associated with a granulitic belt of the Imataca Complex, which extends from Río Caura to the delta of the Orinoco River. The deposits are grouped under two categories: lateritic (Cerro Bolívar-type) and metamorphic (El Pao-type). Other iron deposits occur in the Paleogene of the Andean Cordillera and in the Mesozoic of the Caribbean Mountain System.

The most important lateritic Cerro Bolívar-type deposits are Real Corona, El Trueno, Cerro Bolívar, Cuadrilátero Ferrífero de San Isidro, Altamira, and Redondo, with the main reserves at Cerro Bolívar and Cuadrilátero Ferrífero de San Isidro. These are residual lateritic deposits derived from Late Cretaceous weathering of ferruginous quartzite, mainly hematite (including martite) and quartz. Their thickness ranges from a few centimeters to 10 m and in places up to 25 m. Total reserves are over 2,000 million metric tons of high-grade ore.

The main El Pao-type metamorphic deposits are El Pao, Las Grullas, Piacoa, and La Imperial, but the most important and the only one being exploited is El Pao.

In the Coastal Range, the Capaya-El Dorado deposit is a massive lens of specular hematite of hydrothermal origin emplaced in schist and crystalline limestone of Mesozoic age (Caracas Group). Potential reserves are 400,000 metric tons with 51 percent iron.

In the Andean Cordillera, the Quebrada Arriba deposits are oolitic-type associated with Paleogene clastic sedimentary rocks; common iron minerals are chamosite, siderite, hematite, and goethite.

Most of the iron resources in Colombia are in the La Paz del Rio deposit (77 percent), Cerromatoso deposit (20.5 percent), and other minor deposits (2.5 percent). Iron mineralization is mostly related to oolitic sedimentary deposits of Tertiary age. No banded iron deposits have been found in Colombia, but possibilities for their presence exist on the Guyana Shield to the southeast.

Iron-rich laterite is known near Puerto Carreño (Orinoquía), Cerromatoso (Monte Líbano), and Medellín, but its potential is unknown.

Manganese

The most important manganese deposits of the Southeast Quadrant are in Chile, with minor occurrences of manganese mineralization in Argentina and Venezuela. In Venezuela, small isolated manganese occurrences are known in the Precambrian Imataca Complex on the Guyana Shield, the most important being that of Guacuripia. The San Cristobal and Cerro de la Esperanza deposits are in the La Pastora-Botanamo province and are of residual (lateritic) type.

The manganese deposits in Chile are hosted in backarc volcanic-sedimentary sequences of Early Cretaceous age and distributed along a north-trending belt between parallels 28°19' and 30°30'S lat, adjacent to and east of the iron belt. The most important of these deposits are east of the city of La Serena in the mining districts of Fragua, Corral Quemado, Arrayán, La Liga, El Romero, Talcuna, Lambert, and Escondida (Peebles and Ruiz, 1990) and north of Vallenar (La Negra and Coquimbana mines).

Mineralization consists of lenticular massive bodies of pyrolusite, braunite, psilomelane, manganite, and hausmanite with calcite gangue, which lie in two well-defined stratigraphic levels of gray volcanic sandstone interbedded with andesitic volcanic rocks. These deposits are interpreted to have generated by hydrothermal solutions genetically related to contemporaneous volcanic activity (Peebles and Ruiz, 1990).

In the Altiplano region of northern Chile, important manganese resources emplaced in Tertiary and Quaternary sediment are associated with rhyolitic, dacitic, and andesitic volcanism (Navidad, Huachipato, Lluta, and Abundancia mines). Exploitation has been only on a small scale.

Precious metals

Precious-metal mineralization is widespread and very important in the Southeast Quadrant, and occurs in various geologic environments. In the Venezuelan Guyana, important vein-type gold deposits are emplaced in Proterozoic rocks, such as at El Callao, Vuelvan Caras, and Botanamo. El Callao is the most important because of its long-term activity and high productivity; its reserves are estimated at 5 million metric tons with an average grade of 12 grams/ton. The same tonnage and grade are estimated for gold-bearing veins in the Botanamo and Vuelvan Caras mining districts. Placer gold deposits are also abundant in the Venezuelan Guyana; in 1977, they produced 486,859 g silver, and in 1987, 2,578,413 g.

In Colombia, 80 percent of the gold production comes from placers and the rest from vein-type deposits which provide small- to medium-scale mining in several districts in the Central and Occidental Cordilleras. More recently, new prospects have been located in the region of Guainía in the eastern part of the country.

Placer deposits are in Quaternary alluvial sediment or paleochannels in Tertiary sediment. The most important alluvial gold deposits now being exploited in Colombia are along the Nechi River (Department of Antioquía), San Juan River (Department of Choco), and Saldaña River (Department of Tolima) (Lozano and Buenaventura, 1990).

Vein-type gold deposits in Colombia are related to hydrothermal processes under two main conditions: hot spring systems, located close to the surface in volcanic

regions, and deep convecting circulation systems. Most of the gold veins in the Central and Occidental Cordilleras are related to Tertiary diorite and quartz-diorite intrusions, such as the Mande Batholith and the Manizales and Hatillo Stocks in the northern part of the country (Lozano and Buenaventura, 1990).

Newly found prospects in the region of Guainía are in an area of Precambrian metaconglomerate (conglomerate reefs), an environment similar to that of Jacobina in Brazil and Witwattersrand in South Africa.

Silver production in Colombia is very small; the silver is obtained mostly as a byproduct of gold, copper, lead, and zinc vein-type-deposit mining. Mines with higher silver content are Segovia and Remedios in Antioquía, Vetas, and California in Santander, and Marmato in Caldas and Tolima.

Platinum occurs in placer deposits on the west flank of the Occidental Cordillera, where the deposits form a characteristic province in the valleys of the San Juan and Atrato Rivers. Annual production is approximately 11,000 troy oz.

In eastern Ecuador, placer gold-silver deposits are numerous and widespread on all the alluvial terraces; the gold is probably derived from quartz lenses intercalated with metamorphic rocks of the Cordillera Real (Paladines and San Martín, 1980). Other gold-silver occurrences in Ecuador are in polymetallic vein deposits in the polymetallic subprovince of the Altiplano, genetically associated mostly with moderately silicic Tertiary plutons (Paladines and San Martín, 1980).

Many volcanic centers, including calderas, stratovolcanoes, and dome complexes contain genetically related hydrothermal mineral deposits in the central Andes, mainly in the Neogene and Quaternary volcanic complex of southern Peru, southwestern Bolivia, northern Chile, and northwestern Argentina. The most important of these deposits are epithermal gold-silver deposits in southern Peru and northern Chile and polymetallic tin deposits in the central and southern parts of the Bolivian Tin Belt (Ericksen, 1988).

In southern Peru, silver and gold are found mostly in low-sulfur epithermal vein systems, typical of the districts of Cailloma, Arcata, and Orocopampa (Noble and others, 1990). The deposits are the result of epithermal mineralization associated with pulses of igneous activity during three Neogene intervals at 19, 9.5, and 6 Ma; host rocks are volcanic, of late Oligocene to late Miocene age (Arenas, 1988).

Several important discoveries have been made in these Tertiary and Quaternary volcanic belts in Chile during the past 15 years. Among them are the large El Indio and El Tambo gold deposits in the high Andes east of La Serena. The deposits are hosted by Tertiary volcanic rocks of andesitic (8.2 Ma) to rhyolitic and dacitic (11.4 Ma) composition; the latter is pyroclastic tuff affected by intense hydrothermal alteration. Most of the El Indio ore is derived from enargite-pyrite veins with grades of 6-12 percent of copper, 4-10 grams/ton of gold, and 60-120 grams/ton of silver. Quartz veins contain the richest gold ore (over 100 grams/ton of gold); the Indio Sur vein has produced 3,500 grams/ton of gold (Siddeley and Araneda, 1988). At El Tambo, over 80 percent of the gold is native.

North of El Indio, in the Maricunga precious metal belt of northern Chile (27°30'-26°S lat) dominated by Miocene andesitic volcanism, two partly overlapping gold-silver mineralized subbelts of 24-20 Ma and 14-13 Ma have been recognized. Gold-rich deposits such as Marte, Lobo, Refugio, and Aldebarán, related to deeply eroded andesitic stratovolcanoes, are present in both subbelts, while silver(gold) deposits associated with dome complexes occur in the northern part of the western subbelt (Vila, 1991). Vila reports an aggregate geologic reserve of 350 metric tons (11.15 million oz of gold equivalent) in the Maricunga belt.

Farther to the north, in the Antofagasta region between parallels 24°52' and 25°06'S lat, the epithermal precious-metal deposits of El Guanaco (gold and copper), Cachinal de la Sierra (silver), and El Soldado (silver) are genetically related to a Paleocene and Eocene volcanic arc. The deposits are in caldera-complex rocks and were formed by hydrothermal systems related to the final phase of the caldera evolution (Puig and others, 1988).

In addition to the eastern precious-metal belts, a western gold belt in Chile extending from the vicinity of Talca to La Serena has been recognized. This belt includes important deposits such as in the Mantos de Punitaqui and Andacollo districts. Farther to the north, a belt of silver deposits includes Chañarcillo, which was the most important silver producer in Chile (Ruiz, 1990). In northern Chile, the silver deposits of Huantajaya and Caracoles were also very important producers in the past.

Placer-gold deposits are also widespread in Chile, mainly from Copiapó to southern Chile. The most important deposits are in the Andacollo district in the north, in the alluvial placers of Marga-Marga on the coast of central Chile, Lonquimay, Quilacoya, Carahue, Madre de Díos in southern Chile, and in glacial and fluvioglacial placers of southernmost Chile (Río las Minas, Río del Oro).

In Argentina, in addition to placer-gold deposits in the southern part of the country, vein-type gold-silver mineralization is associated with Tertiary magmatism in several districts; for example, in the Sierra de Famatina. In the main Cordillera south of Mendoza, gold and gold-bearing pollymetallic deposits are known (San Ramón, Tordillo-Cerro de la Virgen, Andacollo district) (Jones, 1991).

Lead-zinc

In contrast with a scarcity in the Northern Andes and Chile, lead-zinc deposits are very important in Peru, Bolivia, and northern Argentina. In Colombia, lead-zinc mineralization is known only in a few prospects not adequately explored or defined. Most are in

hydrothermal veins associated with chalcopyrite and precious metals (Las Nieblas and El Diamante), skarn deposits (Guayabos and Salado Blanco), and massive sulfide deposits (El Roble).

Lead resources have not been evaluated much in Venezuela, although a mineralized zone is known on the Araya-Paria Peninsula associated with metasedimentary rocks of Mesozoic age (Tunapi Formation). Zinc occurrences are associated with a Mesozoic metavolcanic sequence in the Caribbean Mountain System (Santa Isabel, State of Guárico) and in the Bailadores deposit in the Andean Cordillera, associated with felsic pyroclastic rocks intercalated with phyllite, turbidite, and crystalline limestone of the late Paleozoic Mucuchachi Formation.

Lead-zinc deposits and ocurrences are known in Ecuador, mainly in the south-central polymetallic districts (Portovelo) and cupriferous districts (Molleturo, Pascuales); mineralization is associated with silver, gold, and copper (Paladines and San Martín, 1980).

Several important lead-zinc deposits and a variety of skarn deposits genetically related to Cenozoic magmatism are strongly concentrated in central Peru, where the Mesozoic sequences contain abundant limestone. They consist mostly of vein and replacement deposits in Mesozoic limestone, but some are veins in Tertiary red beds and volcanic rocks (Petersen, 1990). The most important are Hualgayoc, Quiruvilca, Huanzalá, San Vicente, and Tambo Grande, the last in northernmost Peru.

Numerous lead-zinc deposits in the southern part of the tin-tungsten belt of Bolivia are also important. Some of these are related to the polymetallic tin deposits associated with subvolcanic porphyry intrusions of Miocene age, where a tin-rich core passes outward to lead-zinc and antimony zones. Chikani, Toropalca, and La Española are among the important deposits.

In Argentina, aside from veins containing lead-zinc and silver-bearing minerals, the most important lead-zinc (silver) deposit is that of Sierra Aguilar.

Lead-zinc deposits and occurrences are also known in southern Chile, mainly in the Aysén region, hosted in marl, phyllite, and schist of inferred early Paleozoic age, the most important being Mina Silva. This provided most of Chile's zinc production and 70 percent of the lead production from 1947 to 1962. During the past 15 years, Mina Toqui, emplaced in Early Cretaceous limestone sequences, has been the main producer.

Tin and tungsten

Tin and tungsten deposits of the Southeast Quadrant are concentrated in the unique Bolivian Tin Belt which has provided most of Bolivia's metal production (fig. 4). The belt, in the Cordillera Oriental, extends for about 1,000 km from southernmost Peru to northernmost Argentina, mostly in Bolivian territory (Urquidi-Barrau, 1990). Tin, the country's main product, has played the same role in the national economy of Bolivia as copper has for Chile and Peru.

At the beginning of this century, the grade of tin ore was 12 to 15 percent tin, but it has declined steadily since then. In 1979, most of the mines were extracting ore of slightly less than 1 percent (Rivas, 1979). The deposits are genetically related to Late Triassic to late Tertiary intrusive bodies emplaced in an environment of thick sequences of intensively deformed marine clastic sedimentary rocks of early Paleozoic age.

Two main segments are recognized along the belt, each with different types of deposits and associated intrusive rocks (Rivas, 1979; Urquidi-Barrau, 1990). One segment, north of Oruro, where erosion following Tertiary uplift exposed granitic plutons emplaced in the Late Triassic and Oligocene and Miocene, contains mostly tin and tungsten mineral veins. A second segment, south of Oruro, where polymetallic tin deposits associated with subvolcanic intrusions of Miocene age predominate, lacks tungsten and bears associated lead-zinc or antimony mineralization. In the northern segment San Rafael (Peru), San José-Amarete, La Fabulosa, Milluni, Caracoles, and Colquiri tin, in Chojilla tin-tungsten, and in Candelaria, Bolsa Negra, Chicote Grande, and Kami tungsten are important deposits. Candelaria was the largest tungsten deposit, being exploited in 1985, with a production of 10 to 15 tons of contained WO_3 per month (scheelite-rich pods containing 3 to 6 percent WO_3) (Urquidi-Barrau, 1990).

The polymetallic tin deposits of the southern segment include San José, Llallagua, Cerro Rico de Potosí (tin-silver), and Chorolque, one of the southernmost of the important tin producers.

Aluminum (bauxite)

The most important resources of aluminum are in Venezuela and Colombia. In Venezuela, bauxite deposits are restricted to the Precambrian Guyana Shield; the principal deposits are Pigiguaos, Los Guaicas, Kamoirán, and Nuria. These are lateritic-type deposits, the product of weathering under tropical conditions. They are grouped into two main categories: Pacaraima-type, resulting from the weathering of ultramafic intrusive rocks into the Roraima Group (Los Guaicas, Kamoirán, and Nuria), and Los Pigiguaos-type, derived from weathering of alkalic granitoids.

In Colombia, the most important deposits are those of Sierra de la Macarena (Meta), the Cuiva Plains (Antioquía), and the Alto Cauca Valley. These deposits parallel the present erosion surface indicating that no important changes in topography have occurred since the beginning of the bauxitization process, supposedly recent. Favorable possibilities for new bauxite deposits lie not only in the Andean region but also in eastern Venezuela (Orinoquía) on Precambrian rocks of the Guyana Shield.

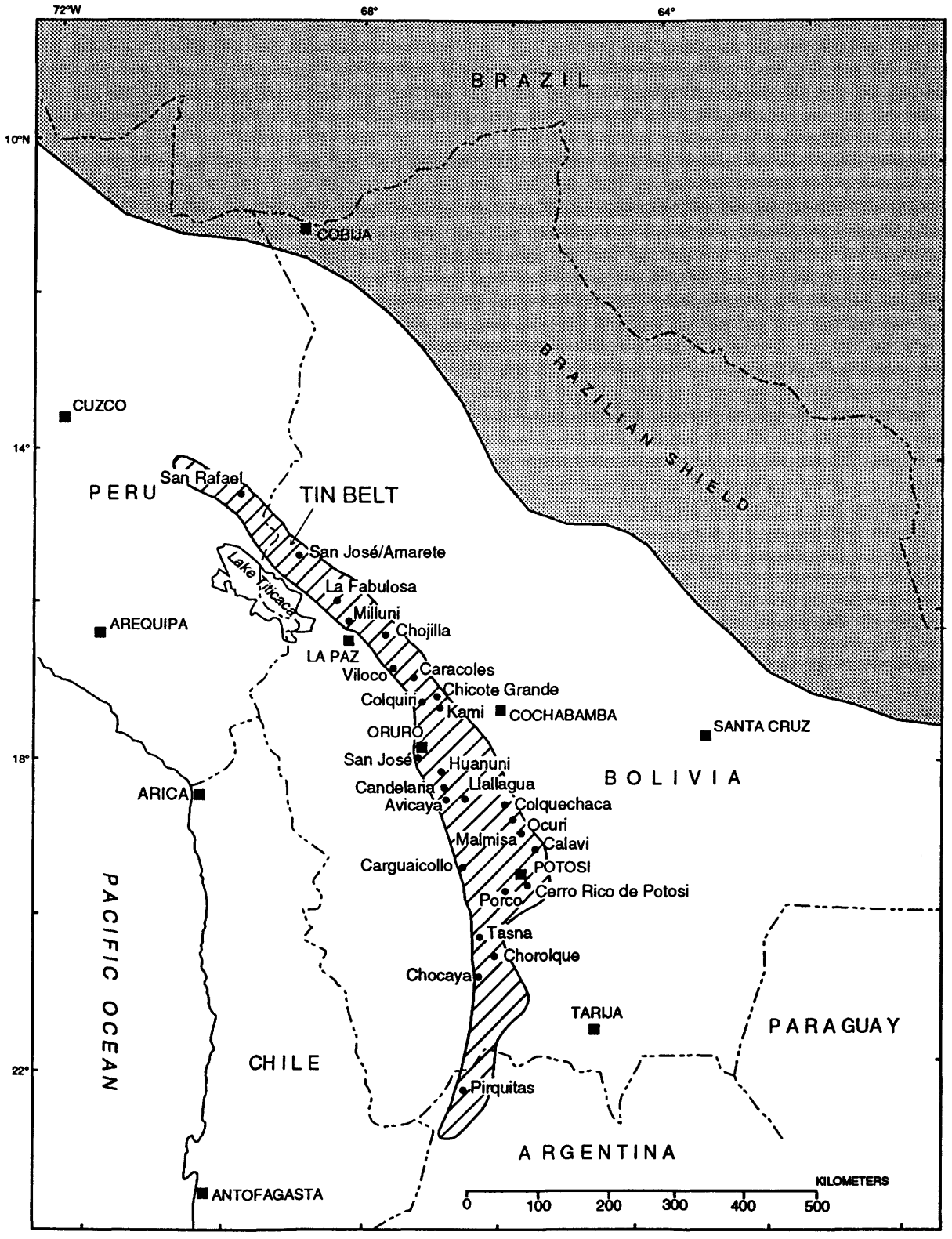

Figure 4. Map showing central Andes Bolivian tin belt (after Lehmann, 1979) and major tin-tungsten, tin, and tin-silver deposits (dots).

Nickel

As with aluminum, the nickel resources of the Southeast Quadrant are in Venezuela and Colombia, in contrast with other mineral resources in the Central Andes.

The most important nickel deposit in Venezuela is that of Loma de Hierro, near Tiara in the Caribbean Mountain System. The deposit is a typical nickeliferous laterite derived from weathering of peridotite and serpentinite of the ophiolitic Loma de Hierro Complex of Early Cretaceous age. The nickel is concentrated in goethite, clay minerals, and garnierite. The thickness of the lateritic cover is about 7 m, locally reaching 15 m. Known reserves are 55 million metric tons with an average grade of 1.53 percent.

Cerromatoso, in Colombia, is a large nickel deposit consisting of nickeliferous laterite derived from the weathering of Cretaceous ultramafic rocks along the Romeral Fault System. Annual production has been 19 million kg. Other minor nickeliferous lateritic deposits in the same geologic environment are those of Planeta Rica, Ure, Morro Pelón, and Ituango.

Lithium

Among the important resources discovered in the Southeast Quadrant during the past two decades is lithium in the salars of the Central Andes (Ericksen and Salas, 1990). Andean salars are known to contain large resources of rock salt, lithium, borax, and smaller resources of gypsum, sodium sulfate, potassium, and magnesium. In many of the 100 basins containing salars or saline lakes in the Central Andean region of western Bolivia, northern Chile, and northwestern Argentina, the salars are zoned and contain the world's most important lithium resources. The largest of these are the Salar de Atacama in Chile, where the first evaluation for lithium was made (Moraga and others, 1974), the Salar de Uyuni in Bolivia, and the Salar del Hombre Muerto in Argentina. The brines of these salars also contain large amounts of recoverable potassium and boron.

Production of lithium started in 1984 at the Salar de Atacama, in an operation designed for annual production of 7,500 tons of lithium carbonate (Ericksen and Salas, 1990). The central halite body of the salar contains the greatest amount of lithium and potassium-rich brine, with an average of 1,800 milligrams/liter of lithium and 28,000 milligrams/liter of potassium. This salt crust has been reported to extend over an area of 1,400 km^2 and to a depth of 426 m; the brines are concentrated in the uppermost porous and permeable 10 m. The resources in the salar nucleus have been estimated at 4.6 million tons of lithium; the total amount contained in dilute saline water within the entire basin may reach twice that amount (Ide and Kunasz, 1990).

In the central part of Salar de Uyuni, within an area of about 2,000 km^2, recoverable lithium-rich (500 milligrams/liter) and potassium-rich brine (10,000 milligrams/liter) have been found in a 5-m-thick porous salt crust.

Brines at the Salar del Hombre Muerto in Argentina are known to contain an average of 700-800 milligrams/liter of lithium and 7,000-8,000 milligrams/liter of potassium over an area of 100 by 150 km with thickness to 15 m.

In the better-studied Salar de Atacama, the lithium is thought to have been derived mainly from the leaching of volcanic rocks and discharged into the salar by stream and groundwater flow (Ide and Kunasz, 1990; Ericksen and Salas, 1990).

Phosphate

Phosphatic rocks have been detected in nearly all the countries in the Southeast Quadrant, but phosphate deposits of economic importance are restricted to Venezuela, Colombia, and Peru.

Occurrences of phosphorite are known in sedimentary sequences accumulated on the continental shelf (or paleoshelf) in open-marine or semirestricted basins of various ages: Ordovician in Bolivia and Argentina; Silurian and Devonian and Triassic in Argentina; Early Jurassic in Peru; Early Cretaceous in Argentina, Chile, and Peru; Late Cretaceous in Venezuela, Colombia, and Ecuador; Miocene in Chile and Peru; and Quaternary in the seafloor sediment on the continental shelf of Peru and Chile (Sheldon and others, 1990).

Economically important phosphorite deposits are found in a well-defined phosphate province in Colombia, Venezuela, and Ecuador, where they occur at several horizons in marine sequences of Late Cretaceous age (Santonian to Maestrichtian?). These correspond to the La Luna Formation and its equivalent in Venezuela and Colombia; the Napo Formation in Ecuador contains only occurrences.

In the Cordillera Oriental of Colombia, phosphate beds are found in the upper part of the La Luna Formation in the Maracaibo Basin; in the Galembo Member of the same formation in the middle part of the Magdalena River Valley, and in the Plaeners Formation in the southernmost part of the phosphate zone (Zambrano-Ortiz and Mojica, 1990). The identified resources are 315 million metric tons with grades ranging from 15 to 25 percent P_2O_5, and 674 million metric tons with 5 to 37 percent P_2O_5.

In Venezuela resources are 18 million metric tons with 3 to 16 percent P_2O_5, 110 million metric tons with 18 percent P_2O_5, 1 million metric tons with 22 percent P_2O_5, all in the La Luna Formation, and 22 million metric tons with 16 percent P_2O_5, in the Navay Formation (Sheldon and others, 1990).

In Peru the most important phosphorite deposit is in the Sechura Basin on the coast, about 800 km north of Lima. Estimated resources are 250 million tons with 25

to 32 percent P_2O_5. Phosphorite in Chile is known in Mejillones (56 million tons with 7 percent P_2O_5) and in an occurrence in the Tongoy area (Sheldon and others, 1990). Igneous apatite occurs in the Coquimbo and Atacama provinces in northern Chile (1 million metric tons with 22 to 26 percent apatite).

SEAFLOOR RESOURCES

Seafloor mineral deposits shown on the map include ferromanganese nodules, hydrothermal sulfide deposits, phosphorites, and heavy-mineral-sand deposits. The information available on sulfide deposits, phosphorites, and heavy-mineral sands is so limited as to preclude estimating abundance; we have merely denoted their locations. Greatest attention has been devoted to the abundance and metal content of nodules.

Nodule abundance (seafloor coverage) at discrete locations has been ascertained from seafloor photographs and sediment cores. The nickel, copper, cobalt, and manganese contents of nodules in many of the core samples and in dredge samples have also been shown. The aim of the ferromanganese nodule section is to explain the procedures used to display these data.

Ferromanganese crust, recovered by dredging, is shown on the map as selected dredge sites. Crusts are divided into four groups, based on their elemental content (Lane and others, 1986; Manheim and Lane-Bostwick, 1989). But information on the occurrence of ferromanganese crust in the region of the Southeast Quadrant is still extremely sparse.

SEAFLOOR SEDIMENT

By
Floyd W. McCoy

Seafloor sediment is classified in four categories by its dominant component: (1) calcareous debris (calcareous ooze/clay or marl), (2) biosiliceous material (biosiliceous ooze/mud/clay), (3) terrigenous clastics (gravel/sand/silt), and (4) clays (including pelagic clay). These 4 sediment types are generalized from the 13-category classification scheme used to depict surficial deposits on the various Circum-Pacific Geologic Maps, a scheme defining 30- and 60-percent boundaries for sediment nomenclature following that devised by Murray and Renard (1891). On the Southeast Quadrant Mineral-Resources Map, a stippled pattern is superimposed where coarse-grained particles (gravel, sand, or coarse-silt sizes) form greater than 15 percent of the sediment (for example, silty or sandy clay, volcanic gravel/sand/silt, calcareous gravel/sand/silt, or biosiliceous silt).

Sedimentary components were identified and abundances estimated via smear-slide analyses of core-top deposits in piston and gravity cores archived at the Lamont-Doherty Earth Observatory. Quantitative control came from analyses of $CaCO_3$ on selected samples. Additional smear-slide and $CaCO_3$ data came from published and unpublished sources. These data formed a primary database for plotting sediment distributions. A secondary database was constructed from general sediment descriptions in the literature that lacked quantitative component and $CaCO_3$ information; this information was used to estimate the geographic extent of distribution patterns. Information from Deep Sea Drilling Project (DSDP) samples were not incorporated because rotary drilling techniques do not recover undisturbed seafloor sediment. Data available at the time of map compilation from Ocean Drilling Program (ODP) sampling by hydraulic piston corers were incorporated. For clastic debris, the Wentworth grade scale was used. Constraints, problems, and assumptions in establishing these databases and using them for mapping are discussed in the various Explanatory Notes pamphlets that accompany each Circum-Pacific Map Project Geologic Map sheet.

For simplification on the Southeast Quadrant Mineral-Resources Map, stations where surficial sediment was sampled or the identification of sediment criteria derived from the primary and secondary databases are not shown; refer to the Southeast Quadrant Geologic Map for this information (Corvalán, 1985b).

Map boundaries of sediment types were controlled by bathymetry, regional water depth of the calcite compensation depth, proximity to land (including knowledge of local geology), and documented seafloor sedimentation processes and deposits, as well as oceanographic and biologic phenomena.

This map depicts unconsolidated sediment recovered primarily by coring and presumably exposed on the ocean floor at the sediment-water interface. This sediment is not necessarily of Holocene age, nor is it necessarily the result of Holocene sedimentary processes.

FERROMANGANESE NODULES

By
David Z. Piper and Theresa R. Swint-Iki

Nodules, consisting mainly of manganese and iron oxides, were first recovered from the Pacific Ocean by HMS *Challenger* during its voyage from 1872 to 1876 (Murray and Renard, 1891). They were most frequently recovered from abyssal depths where the bottom sediment is composed of red clay. Analyses of samples collected during that cruise, as well as of many samples collected subsequently, show content of nickel, copper, and cobalt in the range of a few tenths of 1 percent to about 3 percent. Interest in mining these deposits developed following a series of papers by Mero (1959, 1965), who called attention to the feasibility of their commercial recovery. McKelvey and others (1983)

suggested that molybdenum, vanadium, and several of the rare earth elements might also be recoverable as byproducts of possible future extractions of nickel, copper, and cobalt. These elements, as well as titanium, zinc, barium, lead, strontium, and yttrium, are present in the nodules in the range of ≤ 0.01 to nearly 0.1 percent (McKelvey and others, 1983).

Mero (1965) outlined the features of the geographic distribution of nodules in the Pacific Ocean and the regional variation in their composition. More recent studies include those by Cronan and Tooms (1969), Piper and Williamson (1977), Calvert (1978), Frazer and Fisk (1980), and still others are reported in the compendia of Glasby (1976), Bischoff and Piper (1979), Sorem and Fewkes (1979), and Cronan (1986). Other efforts to delineate the distribution of nodules on maps include those of Ewing and others (1971), Frazer and others (1972), Cronan (1977, 1980), Rawson and Ryan (1978), and McKelvey and others (1979, 1983).

These maps suggest that nodule occurrence and composition in the Pacific Ocean exhibit a rather uniform distribution over areas as great as several thousand square kilometers. Both parameters, however, show uneven variations on the scale of a few tens of square meters. For example, nodule coverage at individual stations near lat 10°N and long 150°W ranges from 0 to greater than 50 percent. Furthermore, coverage at one of these stations, for which 550 photographs were taken while the ship drifted only about 1.5 km, ranges from 0 to 75 percent. Such variability (patchiness) makes it extremely difficult to estimate seafloor coverage on any scale, and particularly at the scale of this map. All maps showing the distribution of abundance and metal content at such scales therefore have a significant degree of uncertainty. Individual data points of nodule abundance and metal content are shown on the map by sets of symbols in order to permit evaluation of the procedures used in the contouring, which are explained below.

Ideally, nodule abundance should be expressed in mass per unit area; for example, kilograms per square meter. Such data, however, are sparse and the abundance is therefore shown in terms of percentage of the sea floor covered. No attempt is made to convert seafloor coverage to mass per unit area for three reasons. (1) Photographs may underestimate the seafloor coverage by as much as 25 percent, because nodules commonly are partly covered by a layer of "fluffy" sediment 5 to 15 mm thick (Felix, 1980). The degree to which they are covered is likely to vary between areas with different seafloor environments and with different nodule morphologies; it varies considerably even between box cores from a single relatively small area. (2) No simple relation exists between nodule cross-sectional area and nodule volume; nodule shapes range from roughly spherical to strongly discoidal (Sorem and Fewkes, 1979). (3) Photographs are taken with the camera nearly on the bottom to as much as several meters above the bottom, thus making it difficult to ascertain accurately the nodule size from the photographs.

Nodules are identified on the bottom photographs as dark and roughly equidimensional objects, with the entire population having a distribution strongly peaked in the size range of 1 to 12 cm in diameter. Angular objects and subrounded objects, often several tens of centimeters across, are identified as rock debris. In most cases, the difference between nodules and rocks is clear. Three people examined all photographs; still some errors in identification may have occurred.

Seafloor coverage of nodules was determined by comparing each photograph with templates showing a light background covered to varying degrees by black objects. The upper limit of 100 percent represents an arrangement of closest packing. The average coverage for all photographs at any one station was plotted as a single point. The number of photographs at a single station ranges from 1 to 850, although for most stations it is between 5 and 15.

Data from sediment cores (including box, gravity, and piston cores) supplement the photographic data. Core stations are plotted merely as recovering or not recovering nodules. Although the core sizes range from half a meter on a side (box cores) to 2.5-cm diameter (gravity cores), integrating these measurements with the photographic data was achieved in the following way.

Areas of varying seafloor coverage of nodules were delineated initially by using only the data obtained from the seafloor photography. A contour of 1 percent was drawn to exclude areas in which photo stations recorded zero coverage. Several sediment cores recovered nodules in these excluded areas, but the coverage outside this contour still is certainly less than 1 percent and probably less than 0.1 percent. The position of the 1-percent contour was further defined by using the core data in two ways: (1) a nodule-bearing core was allowed in the <1-percent area only when its five nearest neighboring cores did not recover nodules, and (2) the contour was drawn to exclude all areas having at least 20 cores, of which 10 percent or fewer recovered nodules. In most areas as large as 12,000 km^2, cores recovering nodules average less than 1 percent of the total number of cores.

The second step was to draw the 50-percent contour to include both photographic stations of greater than 50 percent coverage and areas where recovery of nodules by sampling was greater than 75 percent.

The 10-percent contour was then drawn. This contour encloses photographic stations that show the complete range of coverage. Emphasis was placed, however, on photographic stations that show greater than 25 percent coverage. Some photographic stations that record greater than 25 percent coverage lie outside the 10-percent contour line, if their nearest neighbor records zero percent coverage or if 4 of 5 nearest cores failed to recover a nodule.

The 25-percent contour was drawn lastly to enclose areas of high coverage, supported by either core or photographic data.

The percentage of cores recovering nodules between the 1-percent and 10-percent contours is surprisingly high: within the Northeast Quadrant of the Pacific Ocean, nodule recovery ranged from 8 to 70 percent and averaged 40 percent in areas containing more than 10 cores. These percentages hold true for the Southeast Quadrant as well. In the areas where contours define nodule coverage at 10 to 25 percent, nodule recovery by cores averaged 55 percent and ranged from 25 to 62 percent. For the area of 25 to 50 percent coverage, nodule recovery by cores averaged 64 percent and ranged from 30 to 92 percent. In the area where coverage exceeded 50 percent, nodule recovery by cores averaged 83 percent. One possible explanation for such high recovery by cores is that we have not distinguished between box cores, which sample a relatively large surface area of the sea floor, and gravity and piston cores. Alternatively, seafloor coverage based on bottom photographs may be biased on the low side, owing to sediment cover.

Dredge hauls were not used as a supplement to the photographic and core data because the area sampled by dredging generally is not accurately known.

Nodules were divided according to their chemical composition into four partly overlapping categories: (1) greater than 1.8 percent nickel plus copper, (2) 1.0 to 1.79 percent nickel plus copper, (3) greater than 35 percent manganese, and (4) less than 1.0 percent nickel plus copper (McKelvey and others, 1983). These categories are shown on the map for stations for which data were available in the Scripps Sediment Data Bank. Only one contour, that of 1.8 percent nickel plus copper, is shown, and it is based largely on the data collected and published by McKelvey and others (1979). The problem of contouring the chemical data is similar to that encountered in contouring the coverage data. Small-scale variability precluded exclusion of all conflicting data from the area enclosed by the contour.

Two areas of greater than 50 percent seafloor coverage are delineated by the contours. One area is an east-trending belt of consistently high nodule coverage, centered at 10-15° N. This broad area also corresponds to the area in which the nodules consistently contain more than 1.8 percent nickel plus copper. By contrast, nodules within the second area of high nodule coverage, which is in the Southwest Pacific Basin, contain less than 1.8 percent nickel plus copper. Two additional areas of consistently high coverage occur, one in the Peru Basin and one extending along the south flank of the Pacific-Antarctic Ridge, Southeast Pacific Basin, and Drake Passage.

Nodules and crusts with high cobalt content (these include dredge material) occur in areas of elevated relief, such as seamounts and ridges. In many areas where cobalt-rich nodules are present, ferromanganese crusts of the same composition can exceed 2 cm in thickness (Manheim and Halbach, 1982). Nodules with high manganese content (>35 percent Mn) are restricted within the Southeast Quadrant to the east margin of the Pacific; for example, to the area of near-continent hemipelagic sediment.

The distribution of nodules is strongly related to sediment lithology, shown on the map as a background to the nodule distribution, and to sediment accumulation rates, not shown on this map but included on a 1:17,000,000-scale map of the Pacific Basin (Piper and others, 1985). The distribution of nodules shows a strong preference for siliceous sediment and pelagic clay. They tend not to occur on calcareous sediment, although the west slope of the East Pacific Rise (EPR) at lat 40° to 50°S represents an exception to this generalization. In this and other areas, however, nodules are apparently further restricted to areas exhibiting sediment accumulation rates of less than approximately 5 mm per thousand years (Piper and Swint, 1984; Piper and others, 1987). The Guatemala Basin in the east-central Pacific represents a somewhat unusual region in that nodules have wide distribution in this area of high sediment accumulation. This area has been examined extensively in projects funded by the National Science Foundation (Dymond and others, 1984).

Many factors influence the rather complex patterns of sea-bottom sediment lithology and nodule coverage. These include the supply of material to the seafloor and the secondary processes in the deep ocean that alter or redistribute that supply. The supply is controlled largely by (1) proximity to a source of alumino-silicate material, and (2) primary productivity in the photic zone of the ocean. The source of silicates (clay minerals as well as coarse debris) may be local (marine volcanic activity) or terrigenous (continents contribute material via both rivers and the atmosphere). Primary productivity, on the other hand, controls the "rain" of biogenic detritus to the seafloor. This fraction of organics consists mostly of siliceous and calcareous tests of planktonic organisms, but contains lesser amounts of phosphatic material and organic matter from the soft parts of organisms.

Secondary processes include the dissolution of organic matter at depth in the ocean and the redistribution of sediment by deep-ocean currents. The occurrence of calcareous sediment and the depth of the sea floor show a strong relation, owing to the dissolution of $CaCO_3$ in the deep ocean. This relation can be seen along the EPR in the South Pacific (McCoy, 1985). Calcareous mud predominates along the crest of the rise and down its flanks to a depth of approximately 4,000 to 4,500 m, at which depth it gives way to pelagic clay or siliceous sediment. The exclusion of calcareous debris from the deeper sediment is controlled by the balance between the rate of supply of $CaCO_3$ to the seafloor and its rate of dissolution. The latter increases with water depth, owing to the increase in the solubility of $CaCO_3$ with decreasing water temperature and increasing pressure.

Many measurements of deep-ocean bottom currents have been made, but their usually weak intensity and the complex seafloor bathymetry have combined to thwart attempts to evaluate quantitatively their

importance as a control on sediment accumulation rates and thus indirectly on nodule distribution, except for several careful studies of a few small areas (Lonsdale, 1981).

The origin of nodules is still uncertain after more than 100 years of research. Their distribution in the Pacific Ocean, as shown on this map and the other Circum-Pacific Map Project maps of the Pacific, however, exhibits strong relations to the lithology of surface sediment and to seafloor bathymetry, which may help to elucidate the question of nodule genesis.

Bottom photographs used in this study are from the Bundesanstalt für Geowissenshaften und Rohstoffe, Committee for Co-ordination of Joint Prospecting for Mineral Resources in South Pacific Offshore Areas, Geological Survey of Japan, Hawaii Institute of Geophysics, Institut Français de Recherches pour l'Exploitation de la Mer, Lamont-Doherty Earth Observatory, Kennecott Exploration, Inc., U.S. National Oceanic and Atmospheric Administration, Scripps Institution of Oceanography, Smithsonian Institution, U.S. Navy Electronics Laboratory, and from published literature (Zenkevich, 1970; Andrews and Meylan, 1972; Greenslate and others, 1978). The chemical data on the nodules are from the Scripps Institution of Oceanography Sediment Data Banks.

FERROMANGANESE CRUSTS

By
Frank T. Manheim and Candice M. Lane-Bostwick

The cobalt values indicated on the map represent data normalized to a hygroscopic moisture and substrate (detrital matter)-free basis. The algorithm to obtain these values is given by Co* = Co x 51.23/(Fe+Mn), as determined in Manheim and Lane-Bostwick (1989). Samples designated as being of possible hydrothermal origin are identified by Mn/Fe > 5 and Co < 0.2 percent. Some classes of samples are excluded: data of Barnes (1967) in the Scripps Institution Nodule Data Bank, samples lacking Mn and/or Fe data (which do not permit normalization), and samples having Mn < 5 percent. Multiple samples at one location have been averaged.

The geographical distribution of samples has been largely published in Lane and others (1986). Discussion of the significance of cobalt distribution and of the development of the U.S. Geological Survey Ferromanganese Crust Database is given in Manheim (1986) and Manheim and Lane-Bostwick (1989). The majority of the ferromanganese crust analyses are from two sources; the U.S. Geological Survey World Ocean Ferromanganese Crust Database and the Scripps Institution Nodule Data Bank. Evaluation of these data are discussed in Manheim and Lane-Bostwick (1989). These and other sources are described in Manheim and Lane-Bostwick (1989).

POLYMETALLIC SULFIDES

By
Theresa R. Swint-Iki

The initial discovery of warm-water springs rising from mounds of hydrothermal sediment at the Galapagos spreading center (Corliss and others, 1979; Weiss and others, 1977) and sulfide deposits forming at active high-temperature discharge sites at lat 21°N on the EPR (Spiess and others, 1980) confirmed that hydrothermal circulation at seafloor-spreading axes leads to the precipitation of metal sulfides from hydrothermal fluids strongly enriched in several heavy metals (Von Damm and others, 1985a, 1985b). Several types of seafloor deposits (metal oxides and sulfides) form directly or indirectly from this hydrothermal activity at divergent plate boundaries. Locations of recently discovered deposits through 1993 shown on the map are from Rona and Scott (1993) and Hannington and others (1994).

The thermal balance in oceanic crust along spreading axes is considered to be dominated by hydrothermal circulation and advective cooling, because conductive heat-flow measurements taken along ridge crests consistently show lower than expected values (Lister, 1972; Sleep and Wolery, 1978). Models of hydrothermal processes in oceanic crust developed by Bischoff (1980), Edmond and others (1979a), Fehn and Cathles (1979), Fehn and others (1983), Lister (1977, 1982), and Sleep and Wolery (1978) are largely based on investigations of seafloor-spreading axes in the Northeast Quadrant of the Pacific. Seafloor hydrothermal mineral occurrences are also found along backarc basins, and at intraplate volcanic centers in volcanic and sediment-hosted deposits (Marchig and Gundlach, 1987).

In the Southeast Quadrant, seafloor hydrothermal mineral occurrences are found along the EPR, the Galapagos spreading axis, the south flank of the Costa Rica Rift, and in the Bransfield Strait in the region of the Antarctic Peninsula.

In 1978, divers from a submersible expedition to the EPR at lat 21°N discovered mounds enriched in iron, zinc, and copper sulfides (Francheteau and others, 1979; Hékinian and others, 1980; Spiess and others, 1980). Project Rise returned to the same area in 1979 with the submersible *Alvin* and observed active vents, some discharging fluids at temperatures of 350°C. Additional studies along the EPR at several locations also found evidence of the presence of high-temperature hydrothermal springs. Near lat 11°N on the EPR, massive sulfide mounds and 24 active chimneys were discovered (Ballard and Francheteau, 1980). Dredge hauls at 13°N recovered zinc-rich sulfides like those previously sampled at 21°N (Hékinian and others, 1983). Other study areas where sulfides as chimneys are reported forming on the EPR are shown on the map at lat 17°54'S, lat 18°36'S; lat 20°S, between lat 20°30'S and lat 21°45'S, and further east along the EPR at lat 23°32'S,

long 115°34'W, and lat 26°12.3'S, long 112°36.8'W (Bäcker and others, 1985; Ballard and others, 1981; Marchig and Grundlach, 1987). Recent studies along the southern region of the EPR have revealed many hydrothermal areas. Hydrothermal plumes characteristic of "black smokers" were observed during the Japanese/National Oceanic and Atmospheric Administration (NOAA) VENTS Ridge-Flux Project cruise along the EPR between lat 13°50'S and lat 18°40'S (Feely, 1994). During the *Nautile* on Ultra-fast Ridge (NAUDUR) cruise between lat 17° to lat 19°S, using the submersible *Nautile* along the EPR axis where spreading rates are 141-162 mm/yr, 70 hydrothermal sites with both active and fossil vents were observed (Auzende and others, 1994a, b). The sites are located within three hydrothermal fields on the EPR axis at lat 17°10'S, lat 17°25'S, and in the central zone between lat 18°22'S and 18°34'S. Sediment-hosted deposits have been recovered from cores at DSDP holes 597 and 598 on the west flank of the EPR and also in the region south of the Galapagos spreading axis. Sediment sequences recovered from the Chile Triple Junction at ODP site 863 at lat 46°14'S, long 75°46'W, at the base of the trench slope of the Chile Trench, indicate recent hydrothermal circulation and volcanism (Behrmann, 1992).

Volcanic-hosted deposits have been recovered from cores at DSDP site 504B, approximately 500 km south of the Costa Rica Rift. The recovery of highly altered sulfide-rich stockwork in DSDP core 504B indicates hydrothermal circulation has occurred at this site (Scripps Institution of Oceanography, 1982). Volcanic-hosted deposits have also been recovered from study sites at intraplate volcanic centers in the region of the Society Islands, near lat 18°S, long 148°W (Binard and others, 1991). In the Pitcairn region near lat 25°S, long 127°W, the mineral goethite and amorphous iron were recovered. At Macdonald Seamount, a seafloor volcano in an intraplate setting at lat 28°59'S, long 140°15'W, metalliferous sediment occurs in the summit crater (Cheminée and others, 1991). At lat 63°S, long 60°W, hydrothermally altered sediment is reported in the region of the Antarctic Peninsula, in the Bransfield Strait Basin (Brault and Simmoneit, 1987).

Since the initial observations of phenomenal hydrothermal activity along the Galapagos Rift (Corliss and others, 1979), hydrothermal sulfide deposits have been discovered on each cruise that examined in detail a segment of the EPR (Edmond and others, 1979b; Hékinian and others, 1980; Malahoff, 1982; Normark and others, 1982). Although such deposits are not likely to be continuous along the ridge axis, the entire rise system is considered favorable for their occurrence. Much further work is required to evaluate the extent and composition of seafloor polymetallic sulfide deposits at seafloor-spreading axes, in backarc basins, and at intraplate volcanic centers to evaluate the possible future economic potential of such deposits, as well as to explore for new deposits.

PHOSPHORITES AND PHOSPHATIZED ROCKS

By
David Z. Piper and Theresa R. Swint-Iki

Submarine phosphate deposits consist of rock encrustations, nodules, and pellets. They occur on the continental shelves of Baja California and Peru, on seamounts throughout the central region of the Pacific Basin (for example, the Musicians Seamount Group), and on ridges and seamounts of the continental margin. A dune-beach-nearshore deposit located at Santo Domingo, Baja California, has recently come into production. It averages only 4 percent P_2O_5 but is estimated to have a mean thickness of 20 m over an area of about 1,800 km^2 and to contain 1 to 5 billion tons of P_2O_5. Because it is an unconsolidated sand, it is easy to mine and beneficiate. Plans call for production of about 1.5 million metric tons of concentrate per year (Stowasser, 1982).

No deep ocean seamount deposits are considered to be of commercial interest.

Guano deposits are located on many Pacific Ocean islands, and they represented a major resource in the last century. Of particular importance were the deposits on the Chin-Cha Islands, off the coast of Peru.

HEAVY-MINERAL DEPOSITS

By
Gretchen Luepke

Submerged beaches and river channels are favorable sites in the marine environment for the occurrence of concentrations of heavy minerals (placers) such as gold, platinum, chromite, rutile (TiO_2), and ilmenite ($FeTiO_3$). Beginning with the formation of the great ice sheets during the Quaternary, sea level has repeatedly fallen and risen again by more than 200 m. As a result of sea-level fluctuations, fossil beaches are found both above and below present sea level.

No offshore placer deposits have yet been found off the west coasts of South America or southern Central America. Because of the narrow shelf along most of the west coast of South America, offshore marine placers are probably rare. There are, however, coastal areas with long mining histories where the offshore configuration might be favorable for the formation of placers. Small-scale placer gold mining onshore has occurred since pre-Columbian times in southern Costa Rica and Panama.

Titaniferous magnetite placers occur on beaches from the Golfo de Papagayo in northern Costa Rica to the Peninsula de Osa in southern Costa Rica (U.S. Geological Survey and others, 1987; U.S. Geological Survey, 1994). In addition, ilmenite has been identified at Playa Caldera in Costa Rica. Estimated reserves, where data exist, generally range in the hundred thousand tonnes. The largest deposits occur at Playa

Tarcoles Norte and Playa Bajamar; estimated reserves of magnetite for these deposits are ~2.3 million and ~6.4 million tonnes, respectively (U.S. Geological Survey and others, 1987). On the Peninsula de Osa, three rivers containing gold placers drain into the Golfo Dulce (Roberts and Irving, 1957).

Gold placers have also been worked near the coast in the Provincias of Darién and Veragues in Panama; between 1931 and 1941 exported gold averaged around 5,200 oz per year (Roberts and Irving, 1957). Magnetite and ilmenite placers occur on the coast of the Golfo de Panama between Panama City and the Peninsula de Azuero (U.S. Geological Survey, 1994).

The Department of Nariño in Colombia has the most widespread Quaternary alluvium of any area of the Pacific coast of Colombia and large amounts of gold from Tertiary dioritic and volcanic rocks have been contributed to the rivers of the region (Lozano and Buenaventura, 1990). The southernmost Pacific coast of Colombia may therefore have similar gold-placer potential.

In central Ecuador, four beach deposits have been defined at the mouth of three rivers of the coastal Manabi region. Of three examined deposits, only one, at Cabo Pasado, contained black sand concentrations with high values of iron and titanium: 63.83 percent Fe_2O_3 and 30.20 percent TiO_2 (Carranza-Edwards and others, 1992).

In Chile, gold placers, associated with magnetite, ilmenite, zircon, garnet, and in some places monazite, occur on the west coast of Isla de Chiloé near Pumillahue and Cucao (Ruiz and others, 1965), and also on Isla Ipun. Gold placers of glaciofluvial origin occur on islands, including Islas Picton, Nueva, Lennox, and Navarino, south of the Beagle Canal in Tierra del Fuego (Ruiz and others, 1965).

REFERENCES CITED

Aguirre, L., 1989, Metamorfismo pre-orogénico cretácico y marco geotectónico Cordillera Occidental de Colombia (perfil Bugo-Buenaventura): Revista Geológica de Chile, v. 16, no. 2, p. 123-144.

Aguirre, L., and others, 1974, Andean magmatism: its paleogeographic and structural setting in the central part (30°-35°S) of the southern Andes: Pacific Geology, v. 8, p. 1-38.

Andrews, J.E., and Meylan, M.A., 1972, Results of bottom photography; *Kana Keoki* Cruise Manganese '72, *in* Investigations of ferromanganese deposits from the central Pacific: University of Hawaii Institute of Geophysics Report HIG-72-73, p. 83-111.

Arenas, M.J., 1988, Geological, mineralogical and chemical characteristics of epithermal precious-metal deposits in southern Peru: Revista Geológica de Chile, v. 15, p. 198-200.

Auboin, J.H., and others, 1973, Esquisse paleogéographique et estructurale des Andes Meridionales: Revue de Géographie Physique et de Géologie Dynamique, v. 15, p. 5-72.

Auzende, J.M., and others, 1994a, Observations of present-day activity at super-fast spreading: volcanic, hydrothermal and tectonic studies of the East Pacific Rise (EPR) 17° to 19°S: RIDGE Events, v. 5, no. 1, p. 1-21.

Auzende, J.M., Sinton, J.M., and scientific party, 1994b, *Nautile* on Ultra-fast Ridge (NAUDUR) explorers discover recent volcanic activity along the East Pacific Rise: Eos, v. 75, p. 601.

Bäcker, H., Lange, J., and Marchig, V., 1985, Hydrothermal activity and sulfide formation in axial valleys of the East Pacific Rise crest between 18°S and 22°S: Earth and Planetary Science Letters, v. 72, p. 9-22.

Baldock, J.W., 1982, Geología del Ecuador: Quito, Dirección General de Geología y Minas, 62 p.

Ballard, R.R., and Francheteau, J., 1980, Volcanism and tectonics of the East Pacific Rise and their relationship to hydrothermal circulation: Eos, v. 61, p. 992.

Ballard, R.R., Francheteau, J., Juteau, T., Rangan, C., and Normark, W., 1981, East Pacific Rise at 21°N: the volcanic, tectonic and hydrothermal processes of the central axis: Earth and Planetary Science Letters, v. 55, p. 1-10.

Barnes, S.S., 1967, Minor element composition of ferromanganese nodules: Science, v. 157, p. 63-65.

Behrmann, J.H., and others, 1992, Site 863, *in* Proceedings of the Ocean Drilling Program (ODP); Initial reports: Joint Oceanographic Institutions, Inc., v. 141, p. 343-446.

Bellizzia, A., and Pimentel, N., 1989, Depósitos minerales de Venezuela: tipo, importancia, ambiente geológico asociado y edad de la mineralización: Caracas, Ministerio de Energía y Minas, Dirección de Geología, unpublished report, 29 p.

Binard, N., Hékinian, R., Cheminée, J.-L., Searle, R.C., and Stoffers, P., 1991, Morphological and structural studies of the Society and Austral hotspot regions in the South Pacific: Tectonophysics, v. 186, p. 293-312.

Bischoff, J. L., 1980, Geothermal system at 21°N, East Pacific Rise: physical limits on geothermal fluid and role of adiabatic expansion: Science, v. 213, p. 1465-1469.

Bischoff, J. L., and Piper, D.Z., 1979, Marine geology and oceanography of the Pacific manganese nodule province: New York, Plenum Press, 842 p.

Brault, M., and Simmoneit, B.R.T., 1987, Hydrothermally enhanced diagenetic transformations of biomarker distributions in sediments from the Bransfield Strait, Antarctica:

Eos, Transaction of the American Geophysical Union, v. 68, p. 1769.

Buenaventura, J., 1989, Ocurrencias minerales de Colombia: Bogota, Instituto Nacional de Investigaciones Geológico-Mineras, unpublished report, 20 p.

Calvert, S.E., 1978, Geochemistry of oceanic ferromanganese deposits: Philosophical Transactions of the Royal Society of London, v. 290A, p. 43-73.

Carranza-Edwards, A., Reinoso, H., and Rosales-Hoz, L., 1992, Sedimentological study of beaches from central Ecuador: Review of the Society for Mexican History and Nature, v. 43, p. 15-24.

Cecioni, G., 1957, Cretaceous flysch and molasse in Departamento Ultima Esperanza, Magallanes Province, Chile: American Association of Petroleum Geologists Bulletin, v. 41, p. 538-564.

Cheminée, J.-L., and others, 1991, Gas-rich submarine exhalations during the 1989 eruption of Macdonald Seamount: Earth and Planetary Science Letters, v. 107, p. 318-327.

Corliss, J.B., and others, 1977, Observations of the sediment mounds of the Galapagos Rift during the *Alvin* diving program: Geological Society of America Abstracts with Programs, v. 9, p. 937.

Corliss, J.B., and others, 1979, Submarine thermal springs on the Galapagos Rift: Science, v. 203, p. 1073-1082.

Corvalán, D., J., 1979, Rasgos geológico-estructurales y metalogenéticos relacionados con la segmentación de los Andes: II Congreso Geológico Chileno, Actas, v. 4, p. 45-75.

Corvalán D., J., 1982, Plate-tectonic map of the circum-Pacific region, southeast quadrant: Tulsa, Okla., American Association of Petroleum Geologists, scale 1:10,000,000, 14 p.

Corvalán D., J., 1985a, Geodynamic map of the circum-Pacific region, southeast quadrant: Tulsa, Okla., American Association of Petroleum Geologists, scale 1:10,000,000, 12 p.

Corvalán D., J., 1985b, Geologic map of the circum-Pacific region, southeast quadrant: Tulsa, Okla., American Association of Petroleum Geologists, scale 1:10,000,000, 36 p.

Cronan, D.S., 1977, Deep-sea nodules: distribution and geochemistry, *in* Glasby, G.P., ed., Marine manganese deposits: Amsterdam, Elsevier Publishing Company, p. 11-44.

Cronan, D.S.,1980, Underwater minerals: London, Academic Press, 362 p.

Cronan, D.S., and Tooms, J.S., 1969, The geochemistry of manganese nodules and associated pelagic deposits from the Pacific and Indian Oceans: Deep-Sea Research, v. 16, p. 335-349.

Cronan, D.S., ed., 1986, Sedimentation and mineral deposits in the southwestern Pacific Ocean: London and Orlando, Fla., Academic Press, 344 p.

Drummond, K.J., 1985, Mineral-resources map of the circum-Pacific region, northeast quadrant: Houston, Circum-Pacific Council for Energy and Mineral Resources, scale 1:10,000,000, 48 p.

Dymond, J., and others, 1984, FeMn nodules from MANOP sites H, S, R–control of mineralogical and chemical composition by multiple accretionary processes: Geochimica et Cosmochimica Acta, v. 48, p. 931-949.

Edmond, J.M., and others, 1979a, On the formation of metal-rich deposits at ridge crests: Earth and Planetary Science Letters, v. 46, p. 19-30.

Edmond, J.M., and others, 1979b, Ridge crest hydrothermal activity and the balances of the major and minor elements in the ocean: the Galapagos data: Earth and Planetary Science Letters, v. 46, p. 1-18.

Ericksen, G.E., 1976, Metallogenic provinces of the southeastern Pacific region: American Association of Petroleum Geologists Memoir 25, p. 527-538.

Ericksen, G.E., 1980, Metallogenesis in the Andes, *in* Metallogenesis in Latinoamerica: International Union of Geological Sciences Publication 5, p. 366-374.

Ericksen, G.E., 1988, Hydrothermal deposits in Neogene-Quaternary volcanic centers of the Central Andes: Revista Geológica de Chile, v. 15, p. 204-205.

Ericksen, G.E., and Salas, R., 1990, Geology and resources of salars in the Central Andes, *in* Ericksen, G.E., and others, eds., Geology of the Andes and its relation to hydrocarbon and mineral resources: Circum-Pacific Council for Energy and Mineral Resources Earth Science Series, v. 11, p. 151-164.

Ewing, M., Horn, D., Sullivan, L., Aiken, T., and Thorndike, E., 1971, Photographing manganese nodules on the ocean floor: Oceanology International, v. 6, p. 26-32.

Feely, R.A., and others, 1994, Elemental chemistry of hydrothermal particles along the super-fast spreading southern East Pacific Rise, 13°50' to 18°40'S: Eos, v. 75, no. 44, p. 321.

Fehn, U., and Cathles, L.M., 1979, Hydrothermal convection at slow spreading mid-ocean ridges: Tectonophysics, v. 55, p. 239-302.

Fehn, U., Green, K.E., Van Herzen, R.P., and Cathles, L.M., 1983, Numerical models for the hydrothermal field at the Galapagos Spreading Center: Journal of Geophysical Research, v. 88, p. 1033-1048.

Felix, D., 1980, Some problems in making nodule abundance estimates from sea floor photographs: Marine Mining, v. 2, p. 293-302.

Field, C.W., Wetherell, D.G., and Dash, E.J., 1981, Economic appraisal of Nazca Plate metalliferous sediments, *in* Kulm, L.D., and others, eds., Nazca Plate–crustal formation and Andean convergence:

Geological Society of America Memoir 154, p. 315-320.

Francheteau, J., Juteau, T., and Rangan, C., 1979, Basaltic pillars in collapsed lava-pools on the deep ocean floor: Nature, v. 281, p. 209-211.

Frazer, J.Z., and Fisk, M.B., 1980, Availability of copper, nickel, cobalt, and manganese from ocean ferromanganese nodules (III): Scripps Institution of Oceanography Report SIO 80-16, 117 p.

Frazer, J.Z., Hawkins, D.L., and Arrhenius, G., 1972, Surface sediments and topography of the north Pacific: Scripps Institution of Oceanography, Geologic Data Center, scale 1:3,630,000.

Glasby, G.P., ed., 1976, Marine manganese deposits: Amsterdam, Elsevier Publishing Company, 523 p.

Goossens, P.J., and Rose, W.I., Jr., 1973, Chemical composition and age determination of tholeiitic rocks in the Basic Igneous Complex, Ecuador: Geological Society of America Bulletin, v. 84, p. 1043-1052.

Greenslate, J., Krutein, M., and Pasho, D., 1978, Initial report of the 1972 Sea Scope Expedition: Spokane, Wash., U.S. Bureau of Mines (Minerals Availability System), 3 v.

Guild, P.W., 1981, Preliminary metallogenic map of North America: a numerical listing of deposits: U.S. Geological Survey Circular 858-A, 93 p.

Gursky, J., II, Gursky, M., Schmidt, E., and Wildberg, H., 1985, The geologic development of the ophiolitic basement in southern Central America: Congreso Latinoamericano de Geología, VI, Bogota, 1985, Memorias, Tomo I, p. 31-35.

Hannington, M.C., Petersen, S., Jonasson, I.R., and Franklin, J.M., 1994, Hydrothermal activity and associated mineral deposits of the seafloor: Geological Survey of Canada, Open File 2915-C, scale 1:35,000,000.

Hékinian, R., and others, 1983, East Pacific Rise near 13°N: geology of new hydrothermal fields: Science, v. 219, p. 1321-1324.

Hékinian, R., Ferrier, M., Bischoff, J.L., Picot, P., and Shanks, W.C., 1980, Sulfide deposits from the East Pacific Rise near 21°N: Science, v. 207, p. 1433-1444.

Hervé, F., 1977, Petrology of the crystalline basement of the Nahuelbuta Mountains, south central Chile, *in* Comparative studies in geology: circum-Pacific orogenic belts in Japan and Chile: Tokyo, Japan Society for the Promotion of Science, 1st Report, p. 1-51.

Hughes, F.E., ed., 1990, Geology of the mineral deposits of Australia and Papua New Guinea: Australasian Institute of Mining and Metallurgy Monograph 14, 2 v., 1824 p.

Husman, M.A., Rivera, A., Antunez, E., and Kobe, H.W., 1987, Manto Cobriza: mineralización estratoligada y estratiforme en los sedimentos del Grupo Tarma: Congreso Peruano de Geología, 6th, Lima, 1986, [abs.], p. 117.

Ide, F., and Kunasz, I.A., 1990, Origin of lithium in Salar de Atacama, northern Chile, *in* Ericksen, G.E., and others, eds., Geology of the Andes and its relation to hydrocarbon and mineral resources: Circum-Pacific Council for Energy and Mineral Resources Earth Science Series, v. 11, p. 165-172.

Jones, J.P., 1991, Potencial aurifero de la Republica Argentina: Congreso Geologico Chileno, 6th, Viña del Mar, Chile, 1991, Actas, v. 1, p. 363-367.

Julivert, M., 1973, Les traits structuraux et l'évolution des Andes colombiennes: Revue de Géographie Physique et de Géologie Dynamique, v. 15, p. 143-146.

Lane, C.M., Manheim, F.T., Hathaway, J.C., and Ling, T.H., 1986, Station maps of the world ocean ferromanganese crust database: U.S. Geological Survey Miscellaneous Field Studies Map MF-1869, 2 sheets and pamphlet, scales 1:30,000,000 and 1:5,000,000.

Lehmann, B., 1979, Schichgebundene Sn-Lagerstätten in der Cordillera Real/Bolivien: Berliner Geowissenschaftliche Abhandlungen, Reih A/Band 14, 135 p.

Lister, C.R.B., 1972, On the thermal balance of an oceanic ridge: Royal Astronomical Society Geophysical Journal, v. 26, p. 515-535.

Lister, C.R.B., 1977, Qualitative models of spreading-center processes, including hydrothermal penetration: Tectonophysics, v. 37, p. 203-218.

Lister, C.R.B., 1982, "Active" and "passive" hydrothermal systems in the oceanic crust: predicted physical conditions, *in* Fanning, K.A., and Manheim, F.T., eds., The dynamic environment of the ocean floor: Lexington, Mass., Lexington Books, p. 441-470.

Lonsdale, P., 1981, Drifts and ponds of reworked pelagic sediment in part of the southwest Pacific: Marine Geology, v. 43, p. 153.

Lozano, H., and Buenaventura, J., 1990, Areas of potential new gold deposits in Colombia, *in* Ericksen, G.E., and others, eds., Geology of the Andes and its relation to hydrocarbon and mineral resources: Circum-Pacific Council for Energy and Mineral Resources Earth Science Series, v. 11, p. 173-187.

Malahoff, A., 1982, Massive enriched polymetallic sulfides of the ocean floor; a new commercial source for strategic minerals?: Offshore Technology Conference, 14th, 1982, Proceedings, v. 2, p. 725-730.

Manheim, F.T., 1986, Marine cobalt resources: Science, v. 232, p. 600-608.

Manheim, F.T., and Halbach, P., 1982, Economic significance of ferromanganese crusts on seamounts of the mid-Pacific area: Geological Society of America Abstracts with Programs, v. 14, p. 555.

Manheim, F.T., and Lane-Bostwick, C.M., 1989, Chemical composition of ferromanganese crusts in the world ocean: a review and comprehensive database: U.S. Geological Survey Open-File Report 89-020, 450 p.

Marchig, V., and Gundlach, H., 1987, Ore formation at rapidly diverging plate margins: Results of cruise GEOMETEP 4: Hannover, Bundesanstalt für Geowissenschaften und Rohstoffe Circular 4, p. 3-22.

McCoy, F.W., 1983, Seafloor sediment, *in* Drummond, K.J., Geologic map of the circum-Pacific region, northeast quadrant: Tulsa, Okla., American Association of Petroleum Geologists, scale 1:10,000,000, 40 p.

McCoy, F.W., 1985, Seafloor sediment, *in* Corvalán D., J., Geologic map of the circum-Pacific region, southeast quadrant: Tulsa, Okla., American Association of Petroleum Geologists, scale 1:10,000,000, 36 p.

McKelvey, V.E., Wright, N.A., and Bowen, R.W., 1983, Analysis of the world distribution of metal-rich manganese nodules: U.S. Geological Survey Circular 886, 55 p.

McKelvey, V.E., Wright, N.A., and Rowland, R.W., 1979, Manganese nodule resources in the northeastern equatorial Pacific, *in* Bischoff, J.L., and Piper, D.Z., eds., Marine geology and oceanography of the Pacific manganese nodule province: New York, Plenum Press, p. 747-762.

Mendez, V., and Zappettini, E., 1990, Geology and mineral deposits of the Central Andes, republic of Argentina, *in* Ericksen, G.E., and others, eds., Geology of the Andes and its relation to hydrocarbon and mineral resources: Circum-Pacific Council for Energy and Mineral Resources Earth Science Series, v. 11, p. 195-206.

Mero, J.L., 1959, A preliminary report on the economics of mining and processing deep-sea manganese nodules: Berkeley, University of California Mineral Technology Institute of Marine Research, 96 p.

Mero, J.L., 1965, The mineral resources of the sea: Amsterdam, Elsevier Publishing Company, 312 p.

Moore, G.W., 1982, Plate perimeters and motion vectors, *in* Corvalán D., J., Plate-tectonic map of the circum-Pacific region, southeast quadrant: Tulsa, Okla., American Association of Petroleum Geologists, scale 1:10,000,000, 14 p.

Moraga, A., Chong, G., Fortt, M.A., and Henriquez, H., 1974, Estudio geológico del Salar de Atacama, Provincia de Antofagasta: Instituto de Investigaciones Geológicas (Chile), Boletín 29, 56 p.

Murray, J., and Renard, A.F., 1891, Report on deep-sea deposits based on the specimens collected during the voyage of H.M.S. *Challenger* in the years 1872 to 1876, *in* Thomson, C.W., and Murray, J., eds., Report on the scientific results of the voyage of H.M.S. *Challenger* during the years 1872-1876: New York, Johnson Reprint Corporation, p. 8-147.

Noble, D.C., Eyzaguirre, V.R., and McKee, E.H., 1990, Precious-metal mineralization of Cenozoic age in the Andes of Peru, *in* Ericksen, G.E., and others, eds., Geology of the Andes and its relation to hydrocarbon and mineral resources: Circum-Pacific Council for Energy and Mineral Resources Earth Science Series, v. 11, p. 207-212.

Normark, W.R., Morton, J.L., Koski, R.A., Clague, D.A., and Delaney, J.R., 1982, Active hydrothermal vents and sulfide deposits on the southern Juan de Fuca Ridge: Geology, v. 11, p. 158-163.

North American Metallogenic Map Committee, 1981, Preliminary metallogenic map of North America: U.S. Geological Survey, 4 sheets, scale 1:5,000,000.

Olsson, A., 1942, Tertiary deposits of northwestern South America and Panama: American Science Congress, 8th, Washington, D.C., 1940, Proceedings, v. 4, p. 231-287.

Paladines, A., and San Martín, H., 1980, Mapa metalogénico del Ecuador: Ministerio de Recursos Naturales y Energeticos, Dirección General de Geología y Minas, Ecuador, scale 1:1,000,000.

Palfreyman, W.D., 1995, Mineral-resources map of the circum-Pacific region, southwest quadrant: U.S. Geological Survey Circum-Pacific Map Series, CP-42, scale 1:10,000,000, 66 p.

Park, C., 1961, A magnetite flow in northern Chile: Economic Geology, v. 56, p. 431-441.

Peebles, F., and Ruiz F., C., 1990, Yacimientos de manganeso cretácicos en Chile central: Departamento de Geología y Geofísica, Universidad de Chile, Comunicaciones, no. 41, p. 25-36.

Petersen, U., 1990, Geological framework of Andean mineral resources, *in* Ericksen, G.E., and others, eds., Geology of the Andes and its relation to hydrocarbon and mineral resources: Circum-Pacific Council for Energy and Mineral Resources Earth Science Series, v. 11, p. 213-232.

Piper, D.Z., and Swint, T.R., 1984, Distribution of ferromanganese nodules in the Pacific Ocean: International Geological Congress, 27th, Moscow, 1984, [abs.], v. 3, p. 64.

Piper, D.Z., Swint-Iki, T.R., and McCoy, F.W., 1987, Distribution of ferromanganese nodules in the Pacific Ocean: Chemica Erde, v. 46, p. 171-184.

Piper, D.Z., Swint, T.R., Sullivan, L.G., and McCoy, F.W., 1985, Manganese nodules, seafloor sediment, and sedimentation rates map of the circum-Pacific region, Pacific basin: Tulsa, Okla., American Association of Petroleum Geologists, scale 1:17,000,000.

Piper, D.Z., and Williamson, M.E., 1977, Composition of Pacific Ocean ferromanganese nodules: Marine Geology, v. 23, p. 285-303.

Puig, A., Diaz, S., and Cuitino, L., 1988, Hydrothermal systems related to a Paleogene caldera complex in northern Chile, El Guanaco, Cachinal de la Sierra and El Soldado mining districts, Antofagasta region: Revista Geológica de Chile, v. 15, p. 200-201.

Rawson, M.C., and Ryan, W.B.F., 1978, Ocean floor sediment and polymetallic nodules: New York, Lamont-Doherty Geological Observatory, Columbia University, scale 1:23,230,300.

Rivas, S., 1979, Geology of the principal tin deposits of Bolivia: Geological Society of Malaysia Bulletin 11, p. 161-180.

Roberts, R.J., and Irving, E.M., 1957, Mineral deposits of Central America: U.S. Geological Survey Bulletin 1034, 205 p.

Rodriguez, S.E., 1990, Mineral deposits in the Venezuelan Andes, *in* Ericksen, G.E., and others, eds., Geology of the Andes and its relation to hydrocarbon and mineral resources: Circum-Pacific Council for Energy and Mineral Resources Earth Science Series, v. 11, p. 237-244.

Rona, P.A., and Scott, S.D., 1993, A special issue on sea-floor hydrothermal mineralization: new perspectives: Economic Geology, v. 88, p. 1933-1976.

Ruiz F., C., 1943, Los yacimientos de hierro de la región noroccidental de Copiapó, un tipo no descrito de yacimientos de contacto metamórfico: Sociedad Nacional de Minería, Boletín Minero, no. 522, p. 820-827; no. 523, p. 906-915.

Ruiz F., C., 1961, Exploración por métodos geofísicos aéreos y terrestres de las anomalías ubicadas en la región de cerro Chañar-Boquerón, con una discusión de la génesis de los yacimientos de hierro de Atacama: Santiago, Revista Minerales no. 75, p. 23-30.

Ruiz F., C., 1990, Distribution and characteristics of Chilean copper deposits, *in* Ericksen, G.E., and others, eds., Geology of the Andes and its relation to hydrocarbon and mineral resources: Circum-Pacific Council for Energy and Mineral Resources Earth Science Series, v. 11, p. 245-256.

Ruiz F., C., and Ericksen, G.E., 1962, Metallogenetic provinces of Chile, South America: Economic Geology, v. 57, p. 91-106.

Ruiz F., C., and Lowell, J.D., 1990, Chilean ore deposits and mineral belts: Pacific Rim Congress 90, 2nd, Gold Coast, Australia, 1990, Proceedings, v. 3, p. 275-283.

Ruiz F., C., and others, 1965, Geología y yacimientos metalíferos de Chile: Santiago, Instituto de Investigaciones Geológicas, 305 p.

Sauer, W., 1965, Geología del Ecuador: Quito, Editorial del Ministerio de Educación, 383 p.

Scripps Institution of Oceanography, 1982, On the Costa Rica Rift–*Challenger* drills deep into basement: Geotimes, v. 27, p. 26-28.

Sheldon, R.P., Burnett, W.C., and Ricalde, V., 1990, Geologic occurrence, paleogeography and resources of phosphate rock in the Andean region, *in* Ericksen, G.E., and others, eds., Geology of the Andes and its relation to hydrocarbon and mineral resources: Circum-Pacific Council for Energy and Mineral Resources Earth Science Series, v. 11, p. 257-272.

Siddeley, G., and Araneda, R., 1988, The El Indio and El Tambo gold deposits, Chile: Revista Geológica de Chile, v. 15, p. 201-202.

Sillitoe, R.H., 1976: Andean mineralization: a model for metallogeny of convergent plate margins: Geological Association of Canada Special Paper 14, p. 59-100.

Sillitoe, R.H., 1988, Epochs of intrusion-related copper mineralization in the Andes: Journal of South American Earth Sciences, v. 1, p. 89-108.

Sillitoe, R.H., 1990, Copper deposits and Andean evolution, *in* Ericksen, G.E., and others, eds., Geology of the Andes and its relation to hydrocarbon and mineral resources: Circum-Pacific Council for Energy and Mineral Resources Earth Science Series, v. 11, p. 285-311.

Sleep, N.H., and Wolery, T.J., 1978, Egress of hot water from mid-ocean ridge hydrothermal systems: some thermal constraints: Journal of Geophysical Research, v. 83, p. 5913-5922.

Sorem, R.K., and Fewkes, R.H., 1979, Manganese nodules; research data and methods of investigation: New York, Plenum Press, 723 p.

Spiess, F.N., and others, 1980, East Pacific Rise: hot springs and geophysical experiments: Science, v. 207, p. 1421-1432.

Stowasser, W.F., 1982, Phosphate rock: U.S. Bureau of Mines Minerals Yearbook, Metals and minerals, v. 1, p. 649-666.

Suarez, M., 1977, Aspectos geoquímicos del Complejo Ofiolítico Tortuga en la Cordillera Patagónica del sur, Chile: Revista Geológica de Chile, no. 4, p. 3-14.

Suarez, M., and Pettigrew, T., 1976, An upper Mesozoic island arc-backarc system in the Southern Andes and south Georgia: Geological Magazine, v. 113, p. 305-328.

Sureda, R.J., and Amstutz, G.C., 1981, New investigations on the stratabound Pb-Zn deposits in the Sierra Aguilar, province of Jujuy, Argentina: Zentral Blatt für Geologie und Palaontologie, pt. I, no. 3/4, p. 494-504.

Tavera, F., Maksaev, V., and Chacon, N. (coordinators), 1993, Investigaciones de metales preciosos en el complejo volcánico Neógeno-Cuaternario de los Andes Centrales: La Paz, Bolivia, Proyecto BIC/TC88-02-32-5, 195 p.

Urquidi-Barrau, F., 1990, Tin and tungsten deposits of the Bolivian Tin Belt, *in* Ericksen, G.E., and others, eds., Geology of the Andes and its relation to hydrocarbon and mineral resources: Circum-Pacific Council for Energy and Mineral Resources Earth Science Series, v. 11, p. 313-323.

U.S. Geological Survey, 1994, Titanium in Central America: U.S. Geological Survey Mineral Resource Database System.

U.S. Geological Survey, Dirección General de Geología, Minas e Hidrocarburos, and Universidad de Costa Rica, 1987, Mineral resource assessment of the Republic of Costa Rica: U.S. Geological Survey Miscellaneous Geologic Investigations Series Map I-1865, 75 p.

Vila, T., 1991, Precious metals mineralization styles in the Maricunga Belt, high Andes of northern Chile: Congreso Geológico Chileno, 6th, Santiago, 1991, Actas, v. 1, p. 153-154.

Von Damm, K.L., Edmond, J.M., and Grant, B., 1985a, Chemistry of submarine hydrothermal solutions at Guaymas Basin, Gulf of California: Geochimica et Cosmochimica Acta, v. 49, p. 2221-2237.

Von Damm, K.L., and others, 1985b, Chemistry of submarine hydrothermal solutions at 21°N, East Pacific Rise: Geochimica et Cosmochimica Acta, v. 49, p. 2197-2220.

Weiss, R.F., Lonsdale, P., Lupton, J.E., Bainbridge, A.E., and Craig, H., 1977, Hydrothermal plumes in the Galapagos Rift: Nature, v. 267, p. 600-603.

Yrigoyen, M.R., Corvalán D., J., and Swint-Iki, T.R., 1991, Energy-resources map of the circum-Pacific region, southeast quadrant: U.S. Geological Survey Circum-Pacific Map Series, CP-39, 2 sheets, scale 1:10,000,000, 59 p.

Zambrano-Ortiz, F., and Mojica, P.E., 1990, Characteristics of Colombian phosphate deposits, *in* Ericksen, G.E., and others, eds., Geology of the Andes and its relation to hydrocarbon and mineral resources: Circum-Pacific Council for Energy and Mineral Resources Earth Science Series, v. 11, p. 325-334.

Zenkevich, N.L., 1970, Atlas fotografii dna Tikhogo Okeana: Moscow, Izd-vo Nauka, 134 p.